AGU PUBLICATIONS

Water Resources Research

RESEARCH ARTICLE

10.1002/2015WR018035

Overland flow resistances on varying slope gradients and partitioning on grassed slopes under simulated rainfall

Chengzhong Pan[1], Lan Ma[2], John Wainwright[3], and Zhouping Shangguan[4]

[1]Key Laboratory of Water Sediment Sciences, College of Water Sciences, Beijing Normal University, Beijing, China, [2]Key Laboratory of Soil and Water Conservation and desertification combating, College of Soil and Water Conservation, Beijing Forestry University, Beijing, China, [3]Department of Geography, Durham University, Durham, UK, [4]State Key Laboratory of Soil Erosion and Dryland Farming on the Loess Plateau, Institute of Soil and Water Conservation, Chinese Academy of Sciences, Yangling, Shaanxi, China

Key Points:
- Different relations between resistance and slope gradient exist on granular and grassed surfaces
- The resistance contribution in grass plots follows leaves>stems>litter>soil grain
- Grass plantation greatly increases overland flow resistance and decreases erosion dynamics

Correspondence to:
C. Pan,
pancz@bnu.edu.cn

Citation:
Pan, C., L. Ma, J. Wainwright, and Z. Shangguan (2016), Overland flow resistances on varying slope gradients and partitioning on grassed slopes under simulated rainfall, *Water Resour. Res.*, *52*, 2490–2512, doi:10.1002/2015WR018035.

Received 28 AUG 2015
Accepted 14 MAR 2016
Accepted article online 18 MAR 2016
Published online 1 APR 2016

Abstract It is still unclear how slope steepness (*S*) and revegetation affect resistance (*f*) to overland flow. A series of experiments on runoff hydraulics was conducted on granular surfaces (bare soil and sandpaper) and grassed surfaces, including grass plots (GP), GP with litter (GL), and GP without leaves (GS) under simulated rainfall and inflow ($30<Re<1400$) with varying slopes ranging from 2.6% to 50%. The results show that the observed *f* based on a small-size runoff plot under rainfall conditions tends to be overestimated due to the increase in flow rate, or Re (Reynolds number), with downward cross sections and a good *f*-Re relation ($f = K\mathrm{Re}^{-1}$). There exists a good *f*-Re relation for granular surfaces and a good *f*-Fr relation (Fr, Froude number) for grass plots. A greater *f* occurred at the gentle and steep slopes for the granular surfaces, while *f* decreased with increasing slopes for the grass treatments. The different *f*-*S* relations suggest that *f* is not a simple function of *S*. When $Re\approx1000$, the sowing rye grass with level lines increased *f* by approximately 100 times and decreased bed shear stress to approximately 5%. The contribution of grass leaves, stems, litter, and grain surface to total resistance in the grass plots were averagely 52%, 32%, 16%, and 1%. The greater resistance from leaves may result from the leaves lying at the plot surface impacted by raindrop impact. These results are beneficial to understand the dynamics of runoff and erosion on hillslopes impacted by vegetation restoration.

1. Introduction

It is well known that vegetation can control soil erosion [*Morgan*, 1986], but there is still short of information about the impacting mechanism of vegetation controlling soil erosion under different micro environments (e.g., slope gradients, geomorphological positions) [*Cerdà*, 1998; *Wainwright et al*., 2000; *Gabarrón-Galeote et al*., 2013]. The hydraulic resistance to overland flow could built up a bridge to thoroughly understand the runoff erosion dynamics impacted by vegetation [*Abrahams and Parsons*, 1994; *Gilley and Kottwitz*, 1994]. Hydraulic roughness coefficients are important for calculating flow velocity, water depth, and runoff hydrographs when the Saint Venant equations are used to simulate overland hydrological processes [*Parsons et al*., 1997]. Understanding the hillslope hydrological processes is necessary for the development of process-based erosion models because runoff-driven erosion dynamics, such as shear stress and unit stream power, are always a product of flow velocity, water depth, and slope steepness. The roughness coefficients are sensitive to overland hydrological processes and deserve in-depth investigation [*Abrahams and Parsons*, 1991; *Smith et al*., 2007; *Kim et al*, 2012].

The Darcy-Weisbach resistance factor and Manning coefficients are often used to describe the surface roughness characteristics [*Gilley and Finkner*, 1991; *Smith et al*., 2007]. Due to the consistency in dimensions, Darcy-Weisbach resistance *f* is very popular and often used [*Abrahams et al*., 1986; *Gilley et al*., 1992]. It can be calculated using equation (1) [*Chow*, 1959]:

$$f = \frac{8ghS}{V^2} = \frac{8gqS}{V^3} \tag{1}$$

where *h* is water depth (m), *V* is mean velocity (m s^{-1}), *g* is acceleration due to gravity (m s^{-2}), and *S* is surface slope steepness (%) where no flow acceleration exists, i.e., the surface and bed slopes are parallel, *q* is flow rate (m^2 s^{-1}).

Clearly equation (1) includes the slope steepness variable. Some experiments have highlighted the possible influence of slope steepness on *f*. *Emmett* [1970] found that under 0.3–7.8% slopes and 100<Re<2000, the *f* values varied from 0.1 to 10 for the smooth flume, and from 0.1 to 5.0 for the sand-covered surface with a grain median diameter of approximately 0.5 mm. Emmett also suggested that slope steepness has a positive influence on *f*, but the influence may be fragile due to the considerable observation error. *Savat* [1977] conducted a series of experiments on hydraulic resistance *f* at 5–50% slope steepness on grain soil and sand-covered surfaces and found that *f* increases with increasing *S* by a power equation in a laminar flow regime. However, *Shen and Li* [1973] suggested that slope steepness has no significant effect on *f* for a smooth surface. *Pan and Shangguan* [2007] found that a negative *f*-*S* relation exists on grass-covered plots at 7.8–43.2% slopes. To date, it is still unclear whether a unified *f*-*S* relation exists for granular surfaces or vegetation-covered slopes, or what causes the different *f*-*S* relation under shallow overland flow condition [*Lawrence*, 1997, 2000; *Smith et al*., 2007]).

Inspired by channel or pipe hydraulics, resistance *f* to overland flow is frequently expressed by the Re as follows:

$$f = a\mathrm{Re}^{-b} \tag{2}$$

where *a* and *b* are regressed parameters.

For a laminar flow regime, theoretically, the *b*-value in equation (2) equals 1.0, and equation (2) can be simplified as equation (3).

$$f = K\mathrm{Re}^{-1} \tag{3}$$

where *K* is regressed parameter. *K* equals to 96 for smooth surface under laminar flow regime [*Horton et al*., 1934].

The utility of equations (2) and (3) has been verified by many experiments [*Savat*, 1980; *Roels*, 1984; *Abrahams et al*., 1986]. It means that slope steepness would have no relation with *f* because Re is a product of unit flow rate and kinematical viscosity (υ) (Re=$4q/\upsilon$) and has nothing with *S*.

However, *Abrahams et al*. [1994] argued that equation (2) is not always effective and the *f*-Re relation corresponds to convex or concave curves for some complicated slopes, i.e., vegetation or stone-covered surfaces in desert areas. Furthermore, *f* can be divided into four resistance components when the mobile bed does not occur, and they abide by an additive law (equation (4)) [*Abrahams et al*., 1994; *Hirsch*, 1996]:

$$f = f_{grain} + f_{form} + f_{wave} + f_{rain} \tag{4}$$

where f_{grain} is the friction coefficient attributed to granular roughness, and relates with Re; f_{form} is the friction or drag resistance attributed to form obstacles, i.e., vegetation stems, litter and rock etc.; f_{wave} derives from the dissipation of runoff energy due to water waves which are triggered by topography and flow regimes (Fr); f_{rain} derives from the retarding effect of raindrop impact. The f_{wave} would be affected by slope steepness, which is closely related with Fr, and f_{rain} diminishes with increasing slope steepness [*Savat*, 1977]. Therefore, the resistance *f* is possibly affected by slope steepness.

Additionally, *Lawrence* [1997] proposed a resistance model based on an inundation ratio, defined as the ratio of water depth to roughness height. For a given flow discharge or Re, the varying slope steepness will inevitably trigger a variation in water depth or inundation ratio and further alter *f*.

The above works imply the possible effect of slope steepness on resistance to overland flow. However, there is little detailed data to check or verify these possibilities, especially on vegetated slopes under rainfall conditions.

The unavailability of equation (2) for some complicated slopes [*Abrahams et al*., 1994] hints that the underlying surface characteristics could affect the resistance forming mechanism of overland flow. Grain resistance is commonly a component of complicated surface resistance (equation (4)), and the proportion of grain resistance to total resistance, which is equivalent to the ratio of bed shear stress to total shear stress, is of importance to soil erosion dynamics [*Abrahams and Parsons*, 1991; *Prosser et al*., 1995; *Atkinson et al*., 2000]. For grassed slopes, grass canopy, stems, and litter commonly represent the main resistance components [*Abrahams et al*., 1994], and grass stems tend to receive more attention due to their direct drag

impact on overland flow in laboratory experiments (i.e., *Thompson et al*., 2004; *Ma et al*., 2013]. *Morgan* [1986] summarized Manning roughness coefficient for different types of cultivation, plants, and mulch etc., and suggested that greatest reductions in overland flow velocity occur with dense and spatially uniform vegetation covers. *Weltz et al*. [1992] used computer optimization procedures to identify friction coefficient associated with plant stems and cryptogam surface cover on the interrill area. *Gilley and Kottwitz* [1994] conducted a laboratory study to investigate friction coefficients for typical crops surfaces under different inflow rates ($550<Re<22{,}000$) and found that the hydraulic resistance is influenced primarily by frictional drag over the soil surface, and residue and ground cover on upland agricultural areas. However, there is little information on the contribution of the different grass components to total resistance and its relation with slope steepness under rainfall conditions [*Hirsch*, 1996; *Lawrence*, 2000].

The experiments on flow hydraulics on granular surfaces and grass-plot treatments were conducted on varying slope gradients and simulated rainfall. The objectives of this study are (1) to describe the relation between resistance and slope steepness on granular and grassed plots and elucidate the impact mechanism of slope steepness on the resistances and (2) to partition the contribution of the grain, grass leaves, stems, and litter to total resistance and quantify the effect of grass planting on hydraulic resistance and erosion dynamics. These results would be helpful to clarify the formation of overland flow resistance and to understand the impacting mechanism of grass vegetation on controlling overland flow runoff and erosion dynamics.

2. Materials and Methods

2.1. Experimental Apparatus

The experiments were conducted in an indoor hall for simulating rainfalls. In order to extend the possible effect of rainfall characteristics on overland flow resistance, the two rainfall simulators, including side-sprinkle and pin-head systems were used in this study. The rainfalls were provided by a pair of side-spray nozzle systems or series of grid-array pinheads, and rainfall intensities were adjusted by water pressure and size of nozzle or pinhead [*Xu et al*., 2006]. The rainfall uniformity of the two simulators exceeds 85%. The side-sprinkle rainfall had an intensity of 90 mm h^{-1} with the falling height of 16.0 m, and generated a similar raindrop spectrum to natural storm rainfall with short duration on the loess plateau of China. The drop diameter mainly ranged from 1.0 to 2.5 mm with the kinetic energy of 0.36 J m^{-2} s^{-1}. The pin-head rainfall had a intensity of 30 mm h^{-1} with the falling height of 5.0 m. The pin-head simulator had a relatively even raindrop distribution, and the drop diameter mainly ranged from 1.0 to 1.5 mm with the kinetic energy of 0.18 J m^{-2} s^{-1} [*Xu et al*., 2006].

The experimental flumes or runoff plots were 5.0 m long $\times$ 1.0 m wide $\times$ 0.5 m high, and constructed of plain steel plate and glass plate. The friction resistance to the two lateral sides is negligible due to their large width and the relatively smooth surfaces. The plots were placed on a removable platform with adjustable slopes ranging from 0 to 50%.

Upslope inflow was provided by a rectangular water sink which was located at the upper slope boundary. In order to stabilize the inflow runoff, the sink was separated into the upper and lower parts by a perforated panel. The clear water or slurry was first pumped into the upper part of the sink, and then the stabilized runoff freely flowed over the plot surface from the lower edge of the sink (Figure 1). The inflow rate can be adjusted by pump valves.

2.2. Experimental Design

Two series of trials on granular and grass-plot surfaces were conducted. The granular surfaces included bare soil with little moss (BS), and impermeable sandpaper with 60 meshes (SD). The SD surface had a median grain diameter (d_{50}) of 0.25 mm. The BS surface was covered with 0.25 mm height naturally grown moss (Figure 1), so the BS surface had an equivalent d_{50} to the SD (Table 1).

A loessial loam was packed in the plots to achieve a 30 cm soil layer with approximately 1.25 g cm^{-3} bulk density, and perennial black rye grass (*Lolium perenne* L.) was planted with level row intervals of 20–25 cm for the grass surfaces (Figure 1). In the tested soil, the particles size fractions of <2 μm, 2–25 μm, 25–50 μm, and >50 μm approximately accounted for 11%, 60%, 20%, and 9%, respectively. The grassed plots were subjected to indoor simulated rainfalls when the grass had grown naturally outside for approximately 3

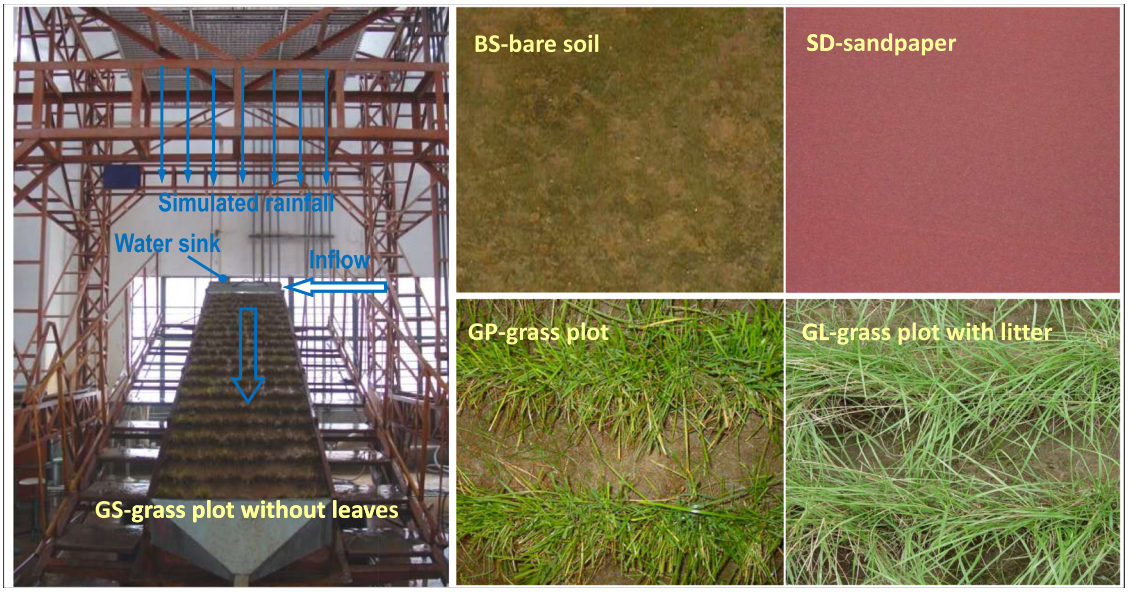

Figure 1. The scheme of this experimental setup and the tested plot surfaces.

months. The grass plot (GP) was covered by the same moss as the BS surface ($d_{50} = 0.25$ mm) and 70% grass cover. The grass plot (GP1) and BS were subjected to 90 mm h^{-1} rainfall, and the slopes varied from 8.7% to 50% (Table 1). When the experiments were performed, the ryegrass belonged to the stage of transition between tillering and jointing periods with a relatively small tillering rate of leaves.

In the later phrase of experiments, some grass dead leaves (i.e., litter) occurred on the grass plot. In order to examine the relative importance of grass different components to resistance, the grass plot (GP2), GL (GP with additional litter), and GS (GP without leaves) were subject to a moderate rainfall with intensity of 30 mm h^{-1} and an upslope inflows with a silt concentration of approximately 25 kg m^{-3} on the slopes of 5.2–25.9% (Table 1 and Figure 1). Grass leaves were clipped and removed from plot surface, to only retain 3 cm height stems to represent GS. The dry weight of the litter and the removed leaves were 72 and 119 g m^{-2}, respectively. In semiarid areas, there was a relatively small runoff rate generated from hillslopes under natural rainfall conditions [*Morgan*, 1986; *Jiang*, 1997], so the inflow rate of 5 and 15 L min^{-1} were assigned to investigate the overland flow resistances.

The raindrop impact on hydraulic resistance became weakened as the slope gradients increased [*Savat*, 1977]. Therefore, the trials at the steeper slopes (i.e., 8.7–50%) were subjected to a greater rainfall of 90 mm h^{-1}, and the trials at the relatively gentle slopes (i.e., 2.6–25.9%) were subjected to a moderate rainfall of 30 mm h^{-1}. The steeper slopes were also used to validate and extent the results drawn from the experiments on the relatively gentle slopes.

Table 1. Trial Treatments on Granular and Grass Plot Surfaces

Treatment	Surface Characteristics	Cover (%)	Slope Gradients	Rainfall Intensity/mm h^{-1}	Inflow Rate/L min^{-1} m^{-1}	Focus[a]
BS	Bare soil covered little moss[b]	0	8.7–50%	90	None	Upslope[c]; f_{grain}
SD1	Sandpaper with $d_{50} = 0.25$ mm	0	2.6–25.9%	30	5	Downslope
SD2	Sandpaper with $d_{50} = 0.25$ mm	0	2.6-25.9%	30	15	Downslope; f_{grain}
GP1	Grass plot	70	8.7–50%	90	None	Upslope
GP2	Grass plot	70	5.2–25.9%	30	15	Downslope; f_{leaves}
GL	Grass plot with litter	70	5.2–25.9%	30	15	f_{litter}
GS	Grass plot with only 3 cm height stems	0	5.2–25.9%	30	15	f_{stems}

[a]Refers to the research focus on the effects of slope positions, and different grass-plot components including leaves, stems, litter, and soil grain beside slope gradients on resistance *f*.
[b]The BS surface has an equivalent median grain diameter (d_{50}) of 0.25 mm.
[c]Upslope and Downslope, respectively, refer to the upper and lower part of a hillslope.

Considering the rainfall runoff gathering effect within a hillslope, the lower part of a hillslope (downslope) tended to correspond to a higher runoff discharge or Re than the upper part (upslope) [*Jiang*, 1997]. Therefore, the trails (i.e., SD, GP2, GL, GS) which were subjected to simultaneously rainfall and inflow can represent the downslope runoff characteristics, while the trials (i.e., BS, GP1) which were subjected to only rainfall can represent the upslope runoff characteristics (Table 1).

2.3. Data Measurement and Analysis

Prior to the experiment, a pilot simulated rainfall was applied to wet each plot and ensure a steady flow state during the observing process. The pilot rainfall had a same intensity as the experimental rainfall, and it lasted for 15–20 min to reach a constant outflow rate for each permeable plot. The experimental duration mainly varied from 20 to 30 min with the exception of the SD1 at 2.6% slope. The exception lasted for 50 min because it took more time to measure surface flow velocity and water depth. The outlet runoff of the plot was collected to ascertain flow rate and sediment concentration if soil erosion occurred.

The 5 m long plot was divided into five 1 m slope segments from up to downslope (i.e., 0–1 m, 1–2 m, 2–3 m, 3–4 m, and 4–5 m), which corresponded to lengthwise cross sections (CSS) of 0.5 m, 1.5 m, 2.5 m, 3.5 m, and 4.5 m. For each slope segment, five or nine measuring stretches paralleled flow direction were set to record stop-watch readings using dye tracer ($KMnO_4$) method (Figure 1). The surface flow velocities (*Vs*) along all stretches were averaged to calculate *Vs* of the slope segment. At the middle (2.5 m) CSS, water depths corresponding to the stretches of flow velocity were recorded via a digital measuring needle with an error of less than 0.04 mm. Water depth was calculated by the elevation difference between ground surface and water surface. Because the measuring needle was easily inserted into soft bases, the water depth was measured more accurately for the sandpaper surface than for the grass plot and bare soil surfaces. Therefore, for the sandpaper surface, mean velocity was first calculated by the volume equation ($V=q/h$), and the correction factor (α) in equation (5) at the 2.5 m cross section was used to extrapolate mean flow velocities at other sections based on the determined *Vs*. For the other surfaces, mean velocity (*V*) was calculated by the measured surface flow velocity (*Vs*) multiplied by a correlation factor α as equation (5):

$$V=\alpha \cdot Vs \tag{5}$$

where α ranges from 0 to 1.0. Judged from the flow Reynolds number, the flow vertical structure was assumed to be a laminar regime, and α was determined to be 0.67 for the bare soil and grass plots [*Horton et al*., 1934].

Under rainfall conditions, due to rainfall runoff and possible infiltration loss, flow rates q at lengthwise cross sections tended to differ from up to downslope. Without considering spatial heterogeneity of soil infiltration and evaporation, q can be calculated using equation (6):

$$q=q_{out}-\left(\frac{q_{out}-q_{in}}{L}\right)\cdot(L-l_s) \tag{6}$$

where q is the flow rate of different cross sections ($m^2\ s^{-1}$), q_{in} and q_{out} refer to the flow rate into and out of plot. L is the total length of the plot or flume (m), $L=5$ m in this study; and l_s is cross section location, expressed as the distance (m) to the upslope end. For impermeable or weakly permeable surfaces, (q_{in}–q_{out})/L can be replaced by rainfall intensity per unit area.

When soil erosion occurs and flurry water flows into the flume, the kinematical viscosity of silt-laden water is adjusted using *Sha* [1965] equation:

$$v_m=\frac{v}{1-\frac{S_v}{2\sqrt{d_{50}}}} \tag{7}$$

where v_m and v are the kinematical viscosity of flurry and clear water, respectively; S_v is the sediment concentration by volume percentage; d_{50} is the sediment grain median particle diameter; and v can be estimated by the measured water temperature.

The Reynolds number (Re), defined as the ratio of inertial forces to viscous forces, can be expressed by equation (8) for both flurry and clear water flow:

Table 2. Surface Flow Velocity (cm s^{-1}) and Its Standard Deviation (S.d) at Each Cross Section

			0–1 m		1–2 m		2–3 m		3–4 m		4–5 m	
Surface	q_{out}[a]/cm^2 s^{-1}	Slope	Mean	S.d	Mean	S.d	Mean	S.d	Mean	S.d	Mean	S.d
Bare soil (BS)	1.0	8.7%	3.0	0.6	6.5	0.6	8.8	2.4	9.5	2.3	13.5	4.3
N = 12[b]	1.0	17.4%	5.0	0.6	8.9	1.0	11.2	3.3	14.2	4.4	18.3	5.5
	1.0	25.9%	5.6	1.1	9.9	1.1	13.1	3.0	16.9	5.8	20.0	6.6
	1.0	34.2%	6.2	1.0	10.8	1.6	14.1	4.2	19.7	7.7	23.2	5.2
	1.0	42.3%	5.8	0.6	10.6	1.0	14.1	2.6	20.3	7.8	26.9	6.1
	1.0	50.0%	5.6	0.9	10.0	1.0	13.1	2.4	16.8	4.6	24.2	6.8
Sandpaper	1.2	2.6%	19.0	12.3	16.8	7.9	19.2	3.2	19.7	3.5	21.4	8.2
(SD1)	1.3	5.2%	19.6	10.2	18.2	5.9	23.1	5.9	23.0	4.2	27.9	5.8
N = 9	1.2	10.5%	49.6	17.1	51.7	28.1	50.6	15.6	51.4	11.6	55.7	6.5
	1.2	15.6%	58.8	19.8	57.8	22.1	54.8	15.2	55.0	16.2	62.7	11.0
	1.2	20.8%	46.5	27.9	48.4	30.6	45.1	24.6	44.3	19.3	53.4	16.1
	1.3	25.9%	52.4	20.0	46.9	17.8	48.2	10.3	59.6	15.8	62.0	10.1
Sandpaper	3.0	2.6%	36.3	5.1	33.3	7.8	35.5	6.5	37.0	4.8	36.9	8.4
(SD2)	2.9	5.2%	39.9	5.7	37.8	3.4	41.6	3.0	41.7	2.6	43.1	5.6
N = 9	2.9	10.5%	84.3	14.1	80.2	10.9	80.2	12.9	78.3	6.2	83.8	8.2
	2.9	15.6%	85.5	16.7	81.3	15.1	74.7	8.2	84.6	10.3	86.4	6.8
	2.9	20.8%	83.7	27.2	78.1	25.2	80.1	20.3	80.8	18.1	86.9	8.5
	2.9	25.9%	80.1	15.4	80.2	14.9	75.4	14.5	81.9	14.7	84.6	9.3
Grass plot (GP1)	1.0	8.7%	1.6	0.1	3.6	0.3	5.5	1.2	6.6	0.4	8.2	2.6
N = 12	1.0	17.4%	2.3	0.1	5.2	0.3	7.4	1.1	8.8	0.9	10.1	1.9
	1.0	25.9%	2.4	0.2	5.7	0.3	7.9	1.2	9.3	1.3	11.9	1.6
	1.0	34.2%	2.7	0.3	6.2	0.3	8.3	1.3	10.4	1.4	12.7	1.6
	1.0	42.3%	3.1	0.5	6.9	0.8	8.8	1.5	10.9	1.5	12.8	1.1
	0.9	50.0%	3.5	0.6	7.4	0.5	9.6	1.6	12.6	2.0	15.1	2.9
Grass plot (GP2)	2.9	5.2%	5.8	1.0	4.7	0.8	4.4	0.7	4.8	0.8	4.9	0.9
N = 15	3.2	10.5%	6.5	1.5	6.2	0.8	5.8	0.8	5.8	0.6	6.1	1.0
	3.1	15.6%	8.9	1.3	7.8	1.4	8.2	1.3	7.6	1.0	8.4	1.7
	3.1	20.8%	8.4	2.1	9.3	1.8	9.9	2.1	8.3	1.5	9.3	1.7
	3.0	25.9%	11.5	3.3	10.3	1.8	12.0	2.2	10.0	1.4	10.2	2.0
Grass plot with litter	2.7	5.2%	4.5	1.1	4.3	0.6	3.9	0.7	3.7	0.8	4.0	0.6
(GL)	2.9	10.5%	6.5	1.2	5.7	1.0	5.9	1.1	5.7	0.8	5.3	0.7
N = 15	2.8	15.6%	8.1	1.7	9.5	2.0	8.1	1.6	7.3	0.8	6.7	0.8
	2.8	20.8%	9.3	2.4	10.4	2.9	9.8	2.0	8.6	1.8	9.3	1.1
	2.0	25.9%	10.0	2.4	10.7	2.2	8.4	1.4	7.9	1.4	8.3	1.4
Grass plot with only stem	3.7	5.2%	8.8	1.2	7.6	1.1	8.1	1.2	7.6	0.9	7.7	0.8
(GS)	3.2	10.5%	9.0	3.0	9.1	1.3	8.9	1.1	8.5	0.9	8.2	1.0
N = 15	3.5	15.6%	12.0	2.2	11.2	1.6	10.9	1.6	10.8	1.8	11.4	2.4
	3.3	20.8%	13.7	2.5	12.6	2.1	12.3	1.8	11.9	1.4	13.9	2.6
	3.5	25.9%	15.2	1.2	14.7	1.9	14.6	1.9	15.3	2.4	15.5	2.3

[a] q_{out} refers to the outlet flow rate of plot.
[b] N refers to the recording number for each cross section.

$$\mathrm{Re} = \frac{\rho_m V h}{\rho \nu_m} \tag{8}$$

where ρ_m and ρ, respectively, refer to the density of flurry and clear water, and ν_m is the kinematical viscosity of flurry water.

Due to the grass roots and moss cover, a negligible erosion rate occurred on the bare soil and grass plots, and the maximum eroded sediment concentration did not exceed 1.0 kg m^{-3} by sampling outflow runoff. For all of the treatments, no visible rills appeared, and the submerged area was almost equivalent to the bed area due to the relatively flat plot surfaces. Analysis of variance (ANOVA) was used to examine the influence of slope gradient and across section on hydraulic characteristics, and multiple comparison was further to classify the homogeneous subsets if there was statistical significance within a group.

3. Results and Analysis

3.1. Overland Flow

3.1.1. Surface Flow Velocity

The measured *Vs* generally increased with increasing *S*. However, for the granular surfaces (i.e., BS, SD1, SD2), the *Vs* changed little when *S* is steeper than 15% (Table 2). Between the different gauging cross sections (CSSs), there was a small variation in *Vs* with exception of BS and GP1 (Table 2).

Table 3. Stepwise Multivariate Regression on Surface Flow Velocity *Vs* and Slope Steepness *S* and Flow Discharge *q*

			$Vs=\beta S^m q^n$					
Treatment	Slope	Flow Rate q/cm^2 s^{-1}	logβ	m	n[a]	R^2	Sig.	N
BS	8.7–50%	0.1–0.9	1.520	0.359	0.616	0.966	<0.001	30
SD1	2.6–25.9%	0.9–1.3	2.085	0.508		0.796	<0.001	30
SD2	2.6–25.9%	2.6–3.0	2.210	0.414		0.841	<0.001	30
SD1+SD2	2.6–25.9%	0.9–3.0	2.030	0.464	0.521	0.86	<0.001	60
BS+SD1+SD2	2.6–50%	0.1–3.0	1.725	0.306	0.923	0.846	<0.001	90
GP1	8.7–50%	0.1–0.9	1.300	0.351	0.687	0.992	<0.001	30
GP2	5.2–25.9%	2.6–3.2	1.302	0.493	–	0.917	<0.001	25
GP1+GP2	5.2–50%	0.1–3.2	1.219	0.348	0.517	0.725	<0.001	55
GL	5.2–25.9%	1.6–2.9	1.316	0.549		0.891	<0.001	25
GS	5.2–25.9%	2.8–3.7	1.090	0.430	0.63	0.917	<0.001	25

[a]Null value for n means that flow discharge q does not enter the equation at $p = 0.05$.

For the impervious or low-infiltration slopes, the additional flow rates due to rainfall gradually increased with the downward CSSs (equation (6)). For instance, for the SD1, the 30 mm h^{-1} rainfall increased runoff rate from 0.25 to 2.25 L min^{-1} m^{-1} corresponding to 0.5 m to 4.5 m CSSs, which accounted for 5% to 45% of the inflow rate of 5 L min^{-1} m^{-1}. Due to the rainfall runoff gathering effect, both *S* and CSS would have effects on the *Vs*, and the ANOVA method was used to discuss their effects.

For BS and GP1 only subjected to simulated rainfalls, both *S* and CSS have a significant effect on *Vs*. However, for the other treatments (i.e., SD1, SD2, GP2, GL, and GS) which were subjected to both inflows and rainfalls, *S* had more effect on *Vs* than CSS, and the contribution of *S* to the total variance in *Vs* exceeded 90%. These results indicated that the measured *Vs* on the upslope under rainfall conditions could not represent the whole slope.

The relationship between flow velocity (*Vs*) and flow rate (*q*), slope steepness (*S*) was regressed by equation (9) [*Emmett*, 1970]:

$$Vs=\beta S^m q^n \text{ or } \log Vs=\log\beta+m\log S+n\log q \tag{9}$$

where β, m and n are the regressed constants. The transformed logarithmic line can be easily obtained using the stepwise multivariate regression analysis (Table 3).

Combining equations (5) and (9) with equation (1), one can obtain equation (10).

$$f=\frac{8ghS}{V^2}=\frac{8gqS}{(\alpha\beta S^m q^n)^3}=\frac{8g}{\alpha^3\beta^3}S^{1-3m}q^{1-3n} \tag{10}$$

From equation (10), if *f* has no relation with *S*, the exponent *m* corresponds to 1/3. *Horton et al*. [1934] suggested that *m* equals 0.33 for a laminar overland flow regime. However, *m* corresponds to 0.3 for a turbulent flow regime based on a constant Manning roughness coefficient. Correspondingly, the discharge exponent *n* should be 0.67 for a laminar regime and 0.4 for a turbulent regime [*Emmett*, 1970].

The *m* values exceed 0.33 except for all the granular surfaces (i.e., BS+SD1+SD2, Table 3), which implies that *S* may have a negative effect on *f* (equation (10)), especially for the grass plot treatments. However, for the treatment (BS+SD1+SD2), a much greater *n* value (0.923) suggests a possibly spurious regression, even if there is an extreme significance ($p < 0.001$, Table 3). For BS, *Vs* at a 50% slope is smaller than those at 42.3% and 34.2% slopes, and so did *Vs* on some CSSs on the GL (Table 2) under the same flow rate. These results indicate that experiential regression analysis sometimes undermines the mechanism recognition [*Holden et al*., 2008].

3.1.2. Flow Hydraulics

Re, for all of the treatments, ranged from 30 to 1400 (Table 4). Judged from the open channel standard, these overland flows should belong to laminar flow condition (Re < 2000). The color dye tracing observation also suggested that these flows should be closer to laminar flow than turbulent flow due to the visible filamental flow lines. Re gradually increased along the downward CSSs due to the rainfall runoff gathering effect (equation (6)).

Fr increased with increasing *S*. Under the similar flow rate, Fr at the 25.9% slope was 3–6 times as much as that at the 5.2% slope for the SD1, SD2, GP2, GL, and GS treatments. Due to the difference in experimental

Table 4. The Experimental Ranges in Flow Hydraulic Characteristics for Each Treatment

Treatment	Slope	q/cm^2 s^{-1}	V/cm s^{-1}	h/mm	Re	Fr	f
BS	8.7–50%	0.1–0.9	2.0–18.0	0.2–1.1	30–310	0.29–2.64	0.48–8.52
SD1	2.6–25.9%	0.9–1.3	5.9–16.7	0.7–1.7	350–550	0.46–1.77	0.47–1.34
SD2	2.6–25.9%	2.6–3.0	13.1–29.4	0.9–2.1	980–1180	0.92-2.99	0.14–0.34
GP1	8.7–50%	0.1–0.9	1.1–10.1	0.4–1.6	30–320	0.11–1.08	3.41–53.40
GP2	5.2–25.9%	2.6–3.2	2.9–8.1	3.3–9.2	960–1180	0.10–0.44	10.63–43.71
GL	5.2–25.9%	1.6–2.9	2.5–7.2	2.4–10.4	610–1090	0.08-0.47	9.42–69.53
GS	5.2–25.9%	2.8–3.7	5.1–10.4	3.1–7.3	990–1400	0.19–0.59	5.95–15.25

conditions, the granular surfaces had the different threshold slope gradients dividing into subcritical (i.e., Fr $<$ 1) and supercritical (i.e., Fr$>$1) flow regimes. The threshold S is 25.9% for BS, and 10.5% for SD. However, due to the additional grass resistance, all the flows for the grass plot treatments belonged to the subcritical flow regimes with the exception of the 4.5 m CSS at the steepest 50% slope (Table 4). For SD, visible roll waves appeared except for on the 2.6% slope. Roll waves were not captured on the other surfaces, which may be due to the relatively low Fr, and high rainfall intensity.

For the BS and GP1 (representing upslope runoff characteristics), Re and Fr significantly increased with the downward cross sections. The Re and Fr values at the 4.5 m cross section were, respectively, 8–10 times and 2–4 times those on the 0.5 m section. This implies that for the overland flow on hillslopes there would be varying flow regimes which closely relate to flow resistance [*Chow*, 1959].

Under the same conditions, statistical analysis showed that the grass plots had significantly ($p = 0.01$) greater f than the granular surface (GP1 versus BS; GP2 versus SD2 at 25.9% slope), and the GL and GP2 had significantly ($p = 0.01$) greater f than the GS.

3.2. The Relationship Between Resistance and Slope Steepness

3.2.1. Granular Surfaces

For BS under 30$<$Re$<$320, as S increased from 8.7% to 50%, f first decreased and then increased, and the minimum f almost corresponded to the 25.9% slope (Figure 2a). For SD under 350$<$Re$<$550 (SD1) and $Re\approx$1000 (SD2), there was a similar f-S relation: f first increased, then decreased and increased again with increasing S, and the minimum f value occurred at the 10.5% slope (Figures 2b and 2c). For all the granular surfaces, S generally had no significant correlation with f with exception of the 2.5 m CSS for SD1 (Table 5). The greater f tended to occur at a gentle (i.e., 5.2–8.7%) or a steep slope (i.e., 25.9–50%) (Figure 2), which implies that there may be a threshold slope gradient corresponding to a minimum f for inundated overland flows.

The multiple comparisons in ANOVA were used to discuss the effect of S and CSS on f (Table 6). For BS, CSS had even greater influence on f than S (Table 6). Multiple comparisons showed that the 0.5 m CSS had a significantly greater f than the 1.5, 2.5, and 3.5 m CSSs, and all of them had a greater f than the 4.5 m CSS; and the lowest and steepest slopes of 8.7% and 50% had a greater f than the other slopes.

For SD1 under 350$<$Re$<$550, due to the relatively great variation in f (Figure 2b), both S and CSS had no significant ($p = 0.05$) effect on f. For SD2 under 980$<$Re$<$1160, S mainly controlled the variance in f compared to CSS, and the slopes of 5.2% and 25.9% corresponded to the greater f than the other slopes. The greater influence of the CSS on f for BS than for SD1 and SD2 indicates that the gauging cross section would have an important impact on f on upslope, rather than on downslope.

3.2.2. Grass Plots

For GP1 under 30$<$Re$<$320, S had no significant ($p = 0.05$) effect on f at 8.7%$<S<$50% (Table 5 and Figure 3). However, for GP2, GL and GS under Re$\approx$1000, S had a significantly negative correlation ($p = 0.01$) with f, and the negative f-S correlation occurred for each cross section (Table 5 and Figure 3).

ANOVA shows that for GP1, CSS had a more significant effect on f ($p < 0.001$) than S. The 0.5 m CSS had a significantly greater f than the others, and the 4.5 m CSS had a smaller f than the 0.5 m and 1.5 m CSSs (Table 6 and Figure 3). The great variability in f with CSSs may be attributed to the low flow discharge or Re due to the limited plot size under the simulated rainfall. However, *Parsons et al.* [1994] suggested that plot size had no clear effect on f on grasslands or shrub lands under the field conditions. The overland runoff flows regularly on the flat plot surfaces in this study, while the flow lines and width altered greatly due to

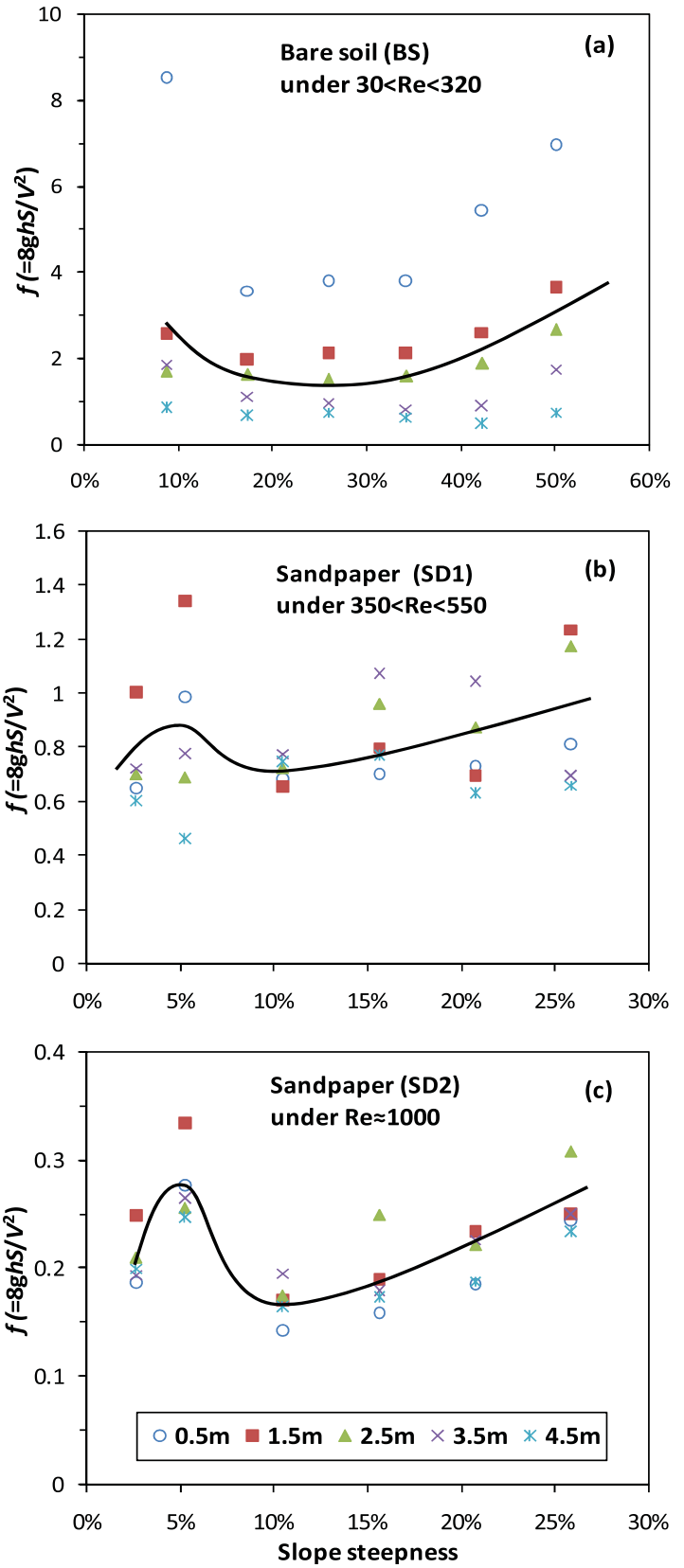

Figure 2. Resistance *f* versus slope steepness for the granular surfaces under the different Re numbers (The solid curves represent the trends of mean values.).

Table 5. Pearson Correlation (R) Between Slope Steepness *S* and Resistance *f* at Each Cross Section

Treatment	Slope	Correlation	*f_0.5m*	*f_1.5m*	*f_2.5m*	*f_3.5m*	*f_4.5m*	*f_all*
BS (Bare soil)	8.7–50%	R	−0.077	0.623	0.699	−0.187	−0.479	0.040
		Sig.	0.884	0.187	0.122	0.723	0.337	0.840
		N	6	6	6	6	6	30
SD1 (Sandpaper)	2.6–25.9%	R	−0.021	−0.125	0.902*	0.292	0.402	0.210
		Sig.	0.968	0.814	0.014	0.575	0.429	0.260
		N	6	6	6	6	6	30
SD1 (Sandpaper)	2.6–25.9%	R	0.014	−0.264	0.515	0.206	−0.037	0.070
		Sig.	0.979	0.614	0.296	0.695	0.945	0.700
		N	6	6	6	6	6	30
GP1 (Grass plot)	8.7–50%	R	−0.808	−0.751	0.653	−0.124	0.124	0.100
		Sig.	0.052	0.085	0.160	0.815	0.815	0.610
		N	6	6	6	6	6	30
GP2 (Grass plot)	5.2–25.9%	R	−0.366	−0.965**	−0.958*	−0.787	−0.868	−0.735**
		Sig.	0.545	0.008	0.010	0.114	0.057	<0.001
		N	5	5	5	5	5	25
GL (grass plot with litter)	5.2–25.9%	R	−0.978**	−0.906*	−0.868	−0.871	−0.942*	−0.794**
		Sig.	0.004	0.034	0.057	0.054	0.016	<0.001
		N	5	5	5	5	5	25
GS (Grass plot with stems)	5.2–25.9%	R	−0.497	−0.985**	−0.594	−0.797	−0.795	−0.634**
		Sig.	0.395	0.002	0.291	0.106	0.108	0.001
		N	5	5	5	5	5	25

* and ** represent the significance at $p = 0.05$ and $p = 0.01$ level, respectively.

the microtopography fluctuation and the covered gravels in the experiments of *Parsons et al*. [1994]. The additional resistance due to topography fluctuations became a dominant component, which would offset the effect of Re on *f* [*Hirsch*, 1996].

For GP2, GL, and GS, *S* had a more significant ($p < 0.001$) effect on *f* than CSS (Table 6). The relatively gentle slopes of 5.2% and 10.5% had greater *f* than the steep slopes of 15.6%–25.9%.

For GP2 and GS where Re≈1000, *f* first increased slightly at 5.2%–10.5% slopes, and then decreased sharply with increasing slopes. The pattern differed from the GL. The smaller *f* at the 5.2% slope than 10.5% for the GP2 and GS may be due to more deposited sediment which filled up part of depressions and smoothed the plot surface [*Pan et al*., 2010]. Nonetheless, the deposited sediment of the gentle slope had a minor effect on the GL surface due to the protruded grass litter.

As *S* increased from 10% to 26% on the grass plots, *f* decreased by 50% for GP2 under Re≈1000 and kept almost constant for GP1 under 30<Re<320 (Figure 3). The different *f*-*S* relations for the GP1 and GP2, as well as for the granular surfaces indicate that the resistance to overland flow is not a function of *S*, and more likely to be affected by other hydraulics.

Table 6. The Effect of Slope Steepness (*S*) and Cross Section (CSS) on Resistance *f* Using Multiple Comparisons in ANOVA

					Homogeneous Subsets[a]		
Surface	Subjects	Levels (Range)	F Value	Sig.	1	2	3
BS	*S*	6 (8.7–50%)	2.98	0.036	17.4–42.3%°	8.7%, 42.3–50%	
	CSS	5 (0.5–4.5 m)	28.10	0.000	2.5–4.5 m	1.5–3.5 m	0.5 m
SD1	*S*	6 (2.6–25.9%)	0.82	0.549	2.6–25.9%		
	CSS	5 (0.5–4.5 m)	2.22	0.103	0.5–4.5 m		
SD2	*S*	6 (2.6–25.9%)	15.03	0.000	2.6%, 10.5–15.6%	15.6–20.8% °	5.2%, 25.9%
	CSS	5 (0.5–4.5 m)	3.83	0.018	0.5–4.5 m		
GP1	*S*	6 (8.7–50%)	1.39	0.271	8.7–50%		
	CSS	5 (0.5–4.5 m)	98.60	0.000	2.5–4.5 m	1.5–3.5 m	0.5 m
GP2	*S*	5 (5.2–25.9%)	14.77	0.000	15.6–25.9%	5.2–10.5%	
	CSS	5 (0.5–4.5 m)	3.00	0.051	0.5–2.5 m, 4.5 m	1.5–4.5 m	
GL	*S*	5 (5.2–25.9%)	32.40	0.000	15.6–25.9%	10.5%	5.2%
	CSS	5 (0.5–4.5 m)	8.73	0.001	0.5–2.5 m	2.5–4.5 m	
GS	*S* s	5 (5.2–25.9%)	13.89	0.000	20.8–25.9%	5.2%,10.5–15.6%	10.5%
	CSS	5 (0.5 m–4.5 m)	4.30	0.015	0.5–2.5 m	1.5–4.5 m	

[a]Homogeneous subsets 1, 2, and 3 (Resistance $f_1 < f_2 < f_3$) are divided based on the observed means for groups at $p = 0.05$ using the Tukey-Kramer method of the multiple comparisons.

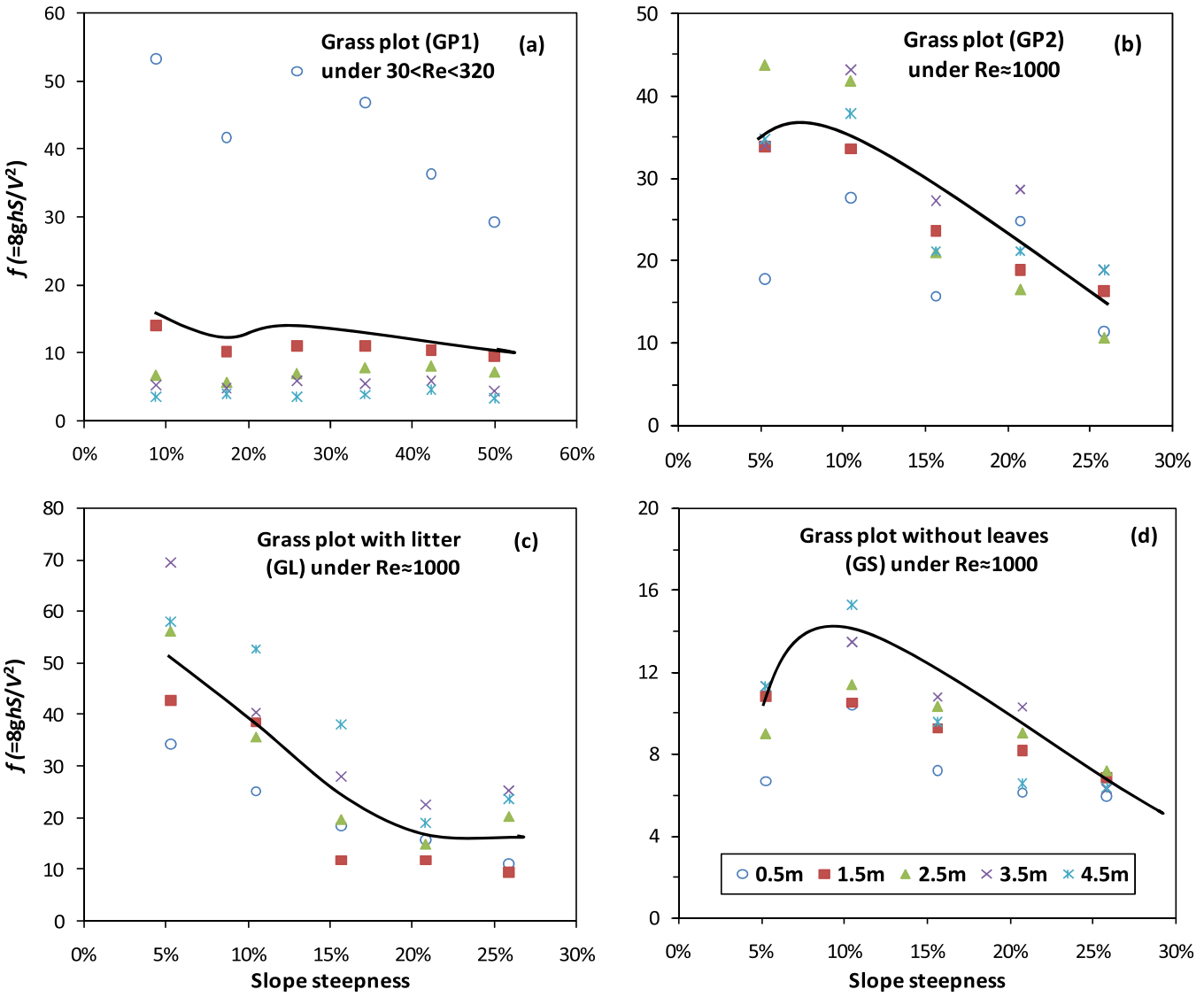

Figure 3. Resistance *f* versus slope steepness for grass plots under the different Re numbers (The solid curves represent the trends of mean values.).

3.3. The Effect of Slope on the Relationship Between Resistance and Re Number

3.3.1. Granular Surfaces

For BS, equation (2) could well describe the *f*-Re relation for each slope steepness, and ANOVA showed that *S* had no significant effect on the *b*-values (ranging from 0.68 to 1.02) in the fitted logarithmic lines ($\log f = \log a - b\log \mathrm{Re}$). Therefore, equation (3) was used to analyze the *f*-Re relation, and all the fitted equations were significant at the $p = 0.01$ level (Figure 4).

The fitted *K* values ranged from 138 to 289, which is approximately 1.5–3.0 times the value (96) for smooth surfaces [*Horton et al.*, 1934], and the gentlest (8.7%) and steepest slope (50%) correspond to a significantly ($p = 0.05$) greater *K* value (289 and 236) than the others (Figure 4).

For SD where $350<\mathrm{Re}<1200$, the *f*-Re relation for each slope steepness was also fitted by equation (3), and each was significant at the $p = 0.01$ level. The fitted *K* values ranged from 280 to 406, which is 2.9–4.2 times the value (96) for a smooth surface, and the maximum *K* value corresponds to the steepest slope (25.9%, Figure 5). The slopes of 5.2% and 25.9% had a significantly greater intercept value (384 and 406) than the other slopes (281–324).

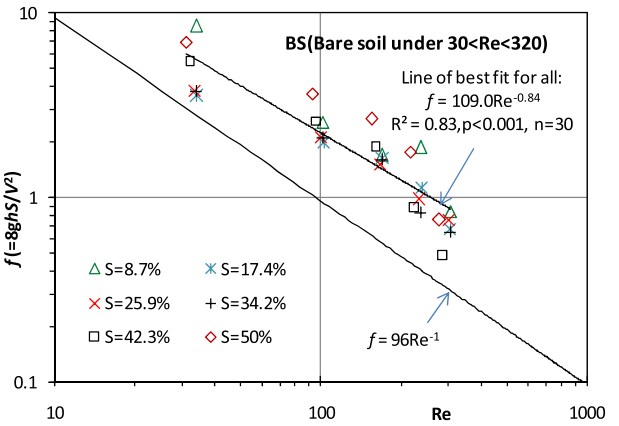

The regressed parameters in $f=K\mathrm{Re}^{-1}$ model

Slope	$f=K\mathrm{Re}^{-1}$			
(%)	K	R^2	Sig.	N
8.7	289.3	0.99	<0.001	5
17.4	137.9	0.92	0.002	5
25.9	143.8	0.94	0.001	5
34.2	143.8	0.94	<0.001	5
42.3	185.5	0.97	<0.001	5
50.0	236.6	0.95	0.001	5
All	190.9	0.89	<0.001	30

Figure 4. Resistance *f* versus Re number at varying slope gradients on the bare soil surface and their regressed equations.

As *S* increases from 10% to 26%, the sandpaper surface generates an increasing *K* value ranging from 290 to 410 under 350<Re<1200, but the bare soil had a decreasing *K* value ranging from 290 to 138 at 10–17% slopes and an almost constant *K* value for 17–26% slopes when 30<Re<320. This indicates that there is no consistent *f*-*S* relation for granular surfaces under different Re conditions.

3.3.2. Grass Plots

For GP1 (30<Re<320), equation (2) could well describe the *f*-Re relation, and the fitted *b* values ranged from 0.90 to 1.21. There was no significant difference ($p = 0.05$) in *b* and log*a* between different slopes (8.7–50%) in the fitted logarithmic lines. This implies that *S* has no significant ($p = 0.05$) effect on the *f*-Re relation on grass plots under low Re values.

Equation (3) was also used to fit the *f*-Re relation, and all of the fitted equations were significant at the $p = 0.01$ level (Figure 6). The *K* values varies from 993 to 1709, which is much greater than that (138–289) of the bare soil (BS) under the same conditions (Figure 4).

For the GP2, GL, and GS treatments under Re≈1000, equations (3) lost its efficacy, and even *f* had an increasing trend with Re. The *f*-Re relation for the GP1 and GP2 corresponds to a concave curve when 30<Re<1200. This result is in line with *Abrahams et al.* [1994], who suggested that the equation $f = a\mathrm{Re}^{-b}$ is not always valid to predict resistance to overland flow, especially on vegetated or stone-covered hillslopes.

3.4. Partitioning Resistance on Grass Plots

3.4.1. The Contribution of Grain Resistance

According to equation (4), the resistance *f* in the grass plots without litter (f_{grass}) mainly derives from the grain surface (f_{grain}) and above-ground grass components when f_{rain} and f_{wave} is negligible due to the 70% grass cover and steep slopes [*Savat*, 1977; *Abrahams et al.*, 1994; *Hirsch*, 1996; *Lawrence*, 2000].

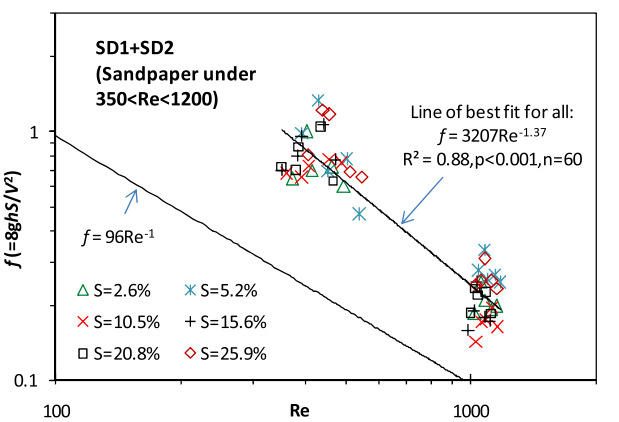

The regressed parameters in $f=K\mathrm{Re}^{-1}$ model

Slope	$f=K\mathrm{Re}^{-1}$			
(%)	K	R^2	Sig.	N
2.6	300.2	0.96	<0.001	10
5.2	384.2	0.93	<0.001	10
10.5	280.7	0.96	<0.001	10
15.6	324.1	0.93	<0.001	10
20.8	304.5	0.95	<0.001	10
25.9	405.5	0.94	<0.001	10
All	329.3	0.93	<0.001	60

Figure 5. Resistance *f* versus Re number at varying slopes (2.6–25.9%) on the sandpaper surface and their regressed equations.

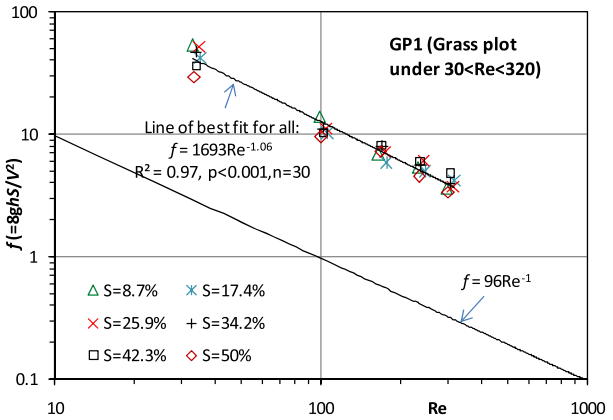

The regressed parameters in $f=KRe^{-1}$ model

Slope	$f=KRe^{-1}$			
(%)	K	R^2	Sig.	N
8.7	1691.3	0.99	<0.001	5
17.4	1421.6	0.99	<0.001	5
25.9	1709.6	0.98	<0.001	5
34.2	1538.5	0.9	<0.001	5
42.3	1233.0	1.00	<0.001	5
50.0	993.9	1.00	<0.001	5
All	1431.5	0.96	<0.001	30

Figure 6. Resistance *f* versus Re number at varying slopes (8.7–50%) on grass plot and their regressed equations.

Because all the treatments had similar grain surface characteristics, under the same rainfall or/and inflow conditions, the *f* obtained from the granular surfaces (BS, SD2) could represent the f_{grain} in the resistance *f* of GP1 and GP2, respectively [*Rauws*, 1988; *Thompson et al.*, 2004]. The f_{BS}, f_{SD2}, f_{GP1}, and f_{GP2}, respectively, represent the hydraulic resistances of BS, SD2, GP1, and GP2, and the contribution of grain resistance to grass plot (f_{grain}/f_{grass}) was, respectively, calculated as (f_{BS}/f_{GP1}) under 30<Re<320 and (f_{SD2}/f_{GP2}) for Re≈1000 (Figure 7).

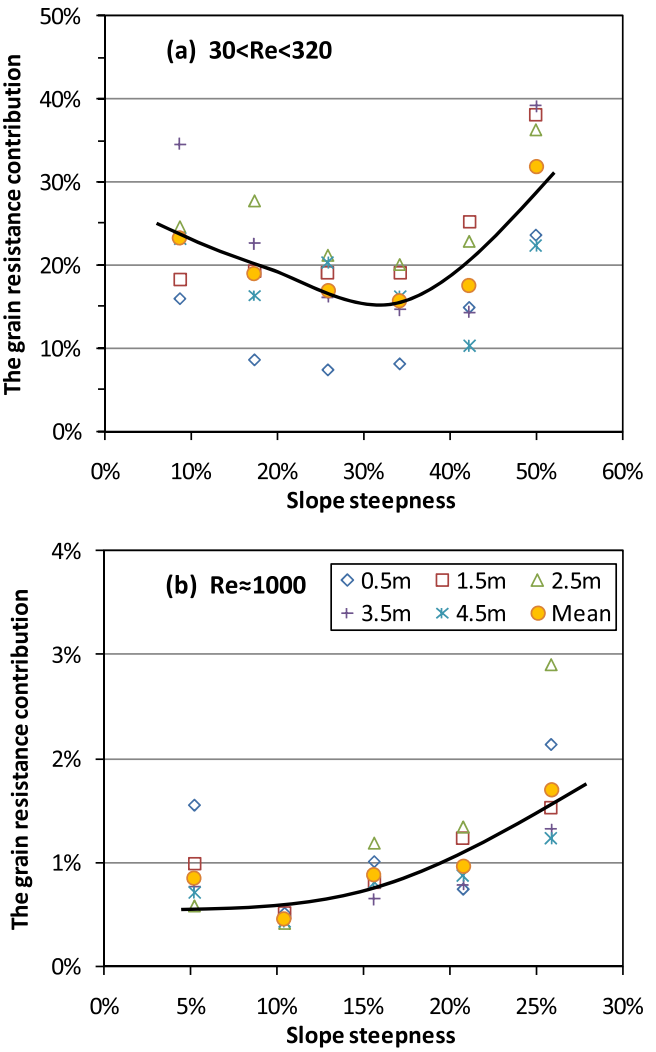

Figure 7. The contribution of grain resistances to the grass plots (f_{grain}/f_{grass}) under (a) 30<Re<320 and (b) under Re≈1000.

Under 30<Re<320, the average value of (f_{grain}/f_{grass}) was 21% at 8.7–50% slopes. This means that grass plantation may add approximately 4 times the resistance of a bare soil surface. The proportion first decreases, and then increases with increasing *S* (Figure 7a). ANOVA shows the 50% slope has a significantly ($p = 0.05$) greater contribution of f_{grain} than the other slopes where no significant difference exists.

Under Re≈1000, the (f_{grain}/f_{grass}) value varied from 0.6% to 2.8% and positively related with *S*. The positive correlation may be mainly due to the decrease in form resistance derived from grass plots with increasing *S* (Figure 3b). At the slopes of 10.5–25.9%, as Re increased from 320 to 1000, the contribution of grain resistance abruptly decreases from approximately 20%–1% (Figure 7).

Furthermore, based on the resistance partitioning, the grain (bed) shear stress (τ_b) on the grass plots was

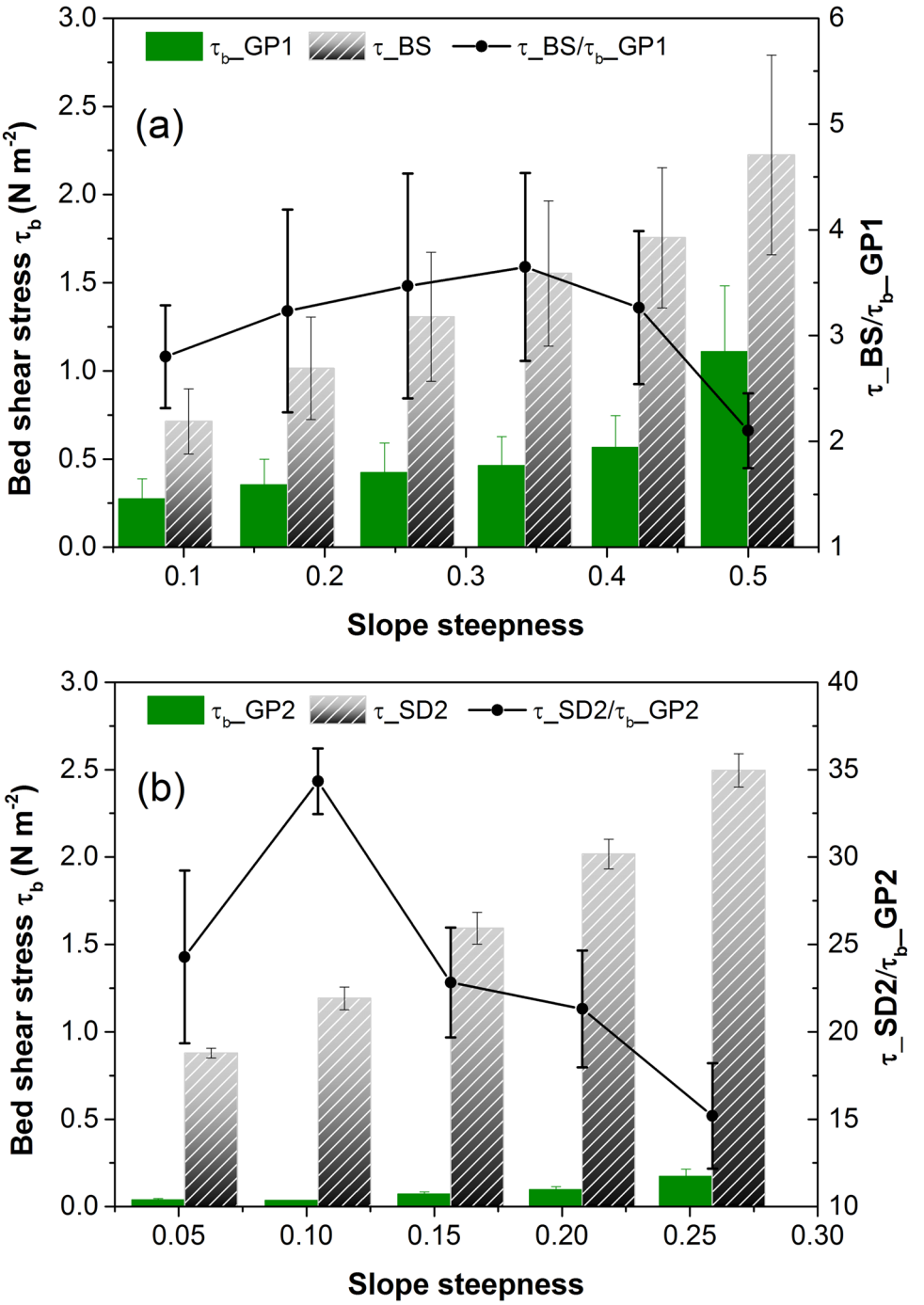

Figure 8. Bed shear stress τ_b for the granular surface and the grass plot (a) under 30<Re<320 and (b) Re≈1000 (τ_b_GP1 and τ_b_GP2 which, respectively, represents bed shear stress for GP1 and GP2 (the same below) are calculated using equation (10), and τ_BS and τ_SD2 refers to total shear stress on the bare soil and sandpaper surface, respectively, which are equivalent to τ_b_BS and τ_b_SD2.)

calculated by the total shear stress (τ) multiplied by (f_{grain}/f_{grass}) as equation (11) [*Rauws*, 1988; *Prosser et al.*, 1995]:

$$\tau_b = \tau(f_{grain}/f_{grass}) = \rho g h S(f_{grain}/f_{grass}) \quad (11)$$

The τ_b is equivalent to total shear stress on granular surfaces. For both the grass plot and granular surfaces, τ_b increased with increasing slopes (Figure 8). This indicates that the increasing slope steepness is prone to soil erosion occurring on both bare soil and vegetated slopes [*Morgan*, 1986; *Fox and Bryan*, 2000].

For the granular surface, τ_b varied from 0.9 to 2.5 N m^{-2} when 30<Re<320 at 8.7–50% slopes, and from 0.7 to 2.2 N m^{-2} when Re≈1000 at 5.2–25.9% slopes. At the same slope of 25.9%, the increment in Re led to the doubled τ_b.

For the grass plot, τ_b varied from 0.3 to 1.1 N m^{-2} when 30<Re<320 at 8.7–50% slopes, and from 0.04 to 0.17 N m^{-2} when Re≈1000 at 5.2–25.9% slopes. At the same slope of 25.9%, the increased Re led to a 60% reduction in τ_b but also had a 4 times increase in τ (from 2.4 to 9.7 N m^{-2}). For each slope steepness, the granular surface correspond to a significantly greater ($p = 0.01$) τ_b than the grass plot. The former were 2–4 times for 30<Re<320 and 15–35 times for Re≈1000 greater than the latter (Figure 8). This implies that the increasing runoff rate or Re would not increase the erosion rate for grassed hillslope. Under the same conditions, the granular surfaces correspond to a significantly greater ($p = 0.01$) τ_b than the grass plots. This result partly explains the effectiveness of vegetated slopes in controlling soil erosion, especially under relatively high Re conditions (i.e., Re≈1000).

3.4.2. The Resistance Components for Grass Plots

Under Re≈1000 conditions, the contribution of the grass components, including stems, litter, and leaves, to total resistance f_{total} was further analyzed under the assumption that these resistance components accord with additive rules [*Weltz et al.*, 1992; *Abrahams et al.*, 1994]:

$$f_{total} = f_{grain} + f_{litter} + f_{stems} + f_{leaves} \tag{12}$$

f_{grain}, f_{stems}, f_{leaves}, and f_{litter} represent the hydraulic resistance caused by grass stems, leaves, litter, and granular bed, respectively, and they can be calculated as $f_{total} = f_{GL}$, $f_{grain} = f_{SD2}$, $f_{litter} = f_{GL} - f_{GP2}$, $f_{stems} = f_{GS} - f_{SD2}$ and $f_{leaves} = f_{GP2}$-f_{GS}.

Just as the total resistance for GL decreased with increasing S (Figure 2c), the f_{stems}, f_{leaves}, and f_{litter} also had a decreasing tendency with S (Figure 9a).

In the four resistance components, grass leaves had the maximum contribution to the total resistance, which accounted for 45–56% with an average of 52%; the secondary one was grass stems which accounted for 18–38% with an average of 31%; the third contributor was grass litter, which accounted for 0 to 34% with an average of 16%; and the grain resistance only covered a 0.5% to 1.5% with an average of 0.7% (Figure 9b). The resistance due to leaves was almost 2 times as much as the resistance due to stems.

4. Discussion

4.1. The Factors Impacting Resistance

The dimensionless variables S, Re, Fr, and $h/(d_{50}/2)$ (the inundation ratio) [*Lawrence*, 1997; *Hirsch*, 1996; *Takken and Govers*, 2000] were selected to discuss the key factors impacting f to overland flow using multivariate regression analysis. The variables related to raindrop impact were excluded because each treatment was subjected to simulated rainfall, and the relatively steep S [*Savat*, 1977]. The relationships between f and these variables are commonly described with a power function [*Hirsch*, 1996; *Lawrence*, 1997], so all of them are transformed into logarithmic form. $h/(d_{50}/2)$ can be replaced by h due to the same grain d_{50} for all treatments.

Compared with h, S and Fr, Re is the most important to all the granular surfaces, and the exponent of Re (0.845∼1.373) is close to 1.0, the theoretical value in a laminar flow regime (Table 7).

For the grass plots under 30<*Re*<320, f also has a close relationship with Re, and the exponent of Re almost equals to 1.0 (Table 7). However, as Re increases (Re≈1000), the $f = K\mathrm{Re}^{-1}$ equation will greatly underestimate f, and f even positively correlates with Re. A threshold Re (approximately 500) corresponds to the minimum f value (2–3, Figure 10a).

For the grass treatments when Re≈1000, Fr has a closer correlation with f than Re, S, and h. In fact, h also has a significantly positive relationship with f under h>2 mm, but has a negative correlation with f under h<2 mm (Table 7 and Figure 10b). This result indicates that Fr, or h, rather than Re, would be suitable variable in predicting f for vegetated hillslopes, especially under relatively high Re values (Re≈1000). This result agrees with *Abrahams et al.* [1994], who found that Re has a negligible effect on f for field grass and shrub hillslopes in a semi-arid area. From the perspective of a resistance forming mechanism, Fr can explain f_{wave},

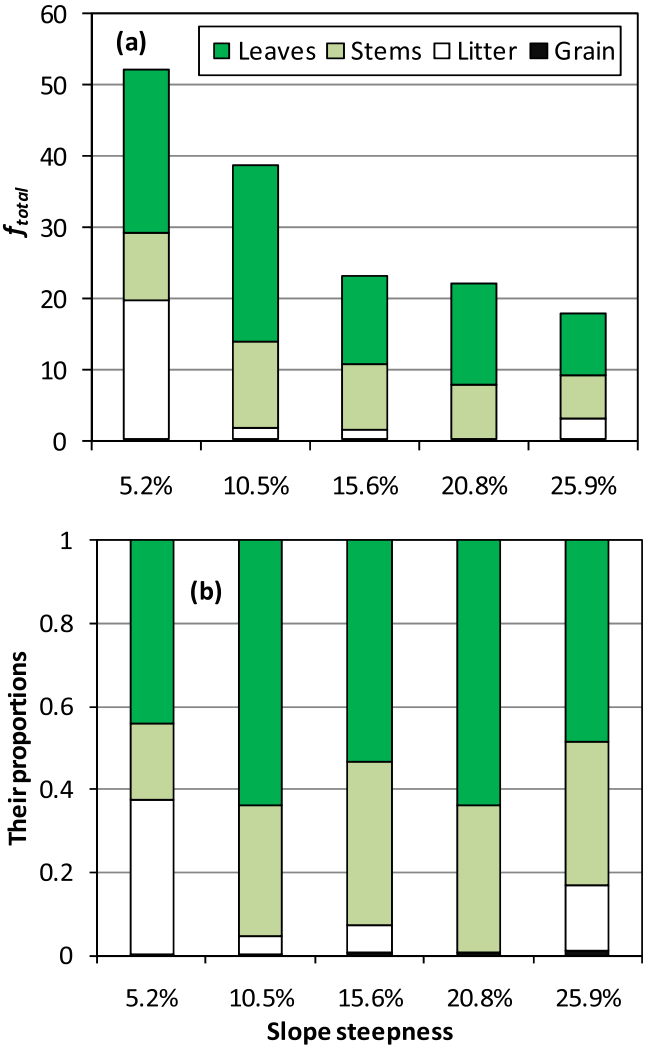

Figure 9. The resistance components (a) and their proportions to the total resistance (the resistance on the grass plot with litter) (b) under Re≈1000 (A small negative value for the litter resistance occurs at 20.8% slope, and it is regarded as naught value.).

and h or $h/(d_{50}/2)$ mainly reflects f_{form}, which closely relates with [*Abrahams and Parsons*, 1994; *Hirsch*, 1996; *Lawrence*, 1997].

The results listed in Table 7 imply that f may be closely related with Re for granular surfaces and with Fr for vegetated slopes, and the effect of S on f would derive from the variation of Fr or h with S (Table 4).

4.2. The Effect of Slope Steepness on Resistance

4.2.1. Granular Surface

For the granular surfaces, the greater f occurred at the gentle or steep slope gradients (Figure 2). The K values in equation (3) (Figures 4 and 5) for different slopes were plotted in Figure 11. *Savat* [1980] also examined the validity of the equation $f = K\mathrm{Re}^{-1}$ for granular surfaces, and suggested that K value increases with S in a laminar flow regime (f-S curve in Figure 11). Obviously, the f-S curve calculated using *Savat* [1980] formula is not in line with this study.

According to equation (3), the average value of K is approximately 330 for SD and 190 for BS (Figures 4 and 5). These are shown as the two level lines (f-Re_1∼2) in Figure 11. So the f-Re relation would not explain the resistance variation across slopes. At the same slope steepness, the greater K value for SD than BS may be related to the visible roll waves occurring on SD. The periodic roll waves tended to increase flow shear stress and augmented the potential of soil erosion [*Liu et al*., 2005].

Lawrence [1997] suggested a resistance model based on the inundation ratio (defined as $h/(d_{50}/2)$). The model included three submodels for different inundation ratios: a drag force submodel for partial

Table 7. Stepwise Multivariate Regression Analysis on Resistance f and Dimensionless Variables Including Slope Steepness S, Re, Fr, $h(h/d_{50}/2)$

Trails	Re	Slope	Variables[a]	Equation	R^2	Sig.	N
BS	30–310	8.7–50%	Re	$\log f = 2.038–0.845\log\mathrm{Re}$	0.833	<0.001	30
SD1+SD2	350–1180	2.6–25.9%	Re	$\log f = 3.506–1.373\log\mathrm{Re}$	0.877	<0.001	60
BS+SD1+SD2	30–1180	2.6–50%	Re	$\log f = 2.296–0.952\log\mathrm{Re}$	0.898	<0.001	90
GP1	30–320	8.7–50%	Re	$\log f = 3.229–1.061\log\mathrm{Re}$	0.966	<0.001	30
GP2	960–1180	5.2–25.9%	Fr	$\log f = 0.758–0.926\log\mathrm{Fr}$	0.849	<0.001	25
GP1+GP2	30–1180	5.2–50%	Fr	$\log f = 0.597–1.152\log\mathrm{Fr}$	0.594	<0.001	55
GL	610–1090	5.2–25.9%	Fr	$\log f = 0.733–0.985\log\mathrm{Fr}$	0.897	<0.001	25
GS	990–1400	5.2–25.9%	Fr	$\log f = 0.701–0.543\log\mathrm{Fr}$	0.770	<0.001	25

[a]The variables refer to first entering the linear logarithmic equation which is very significant at $p = 0.001$.

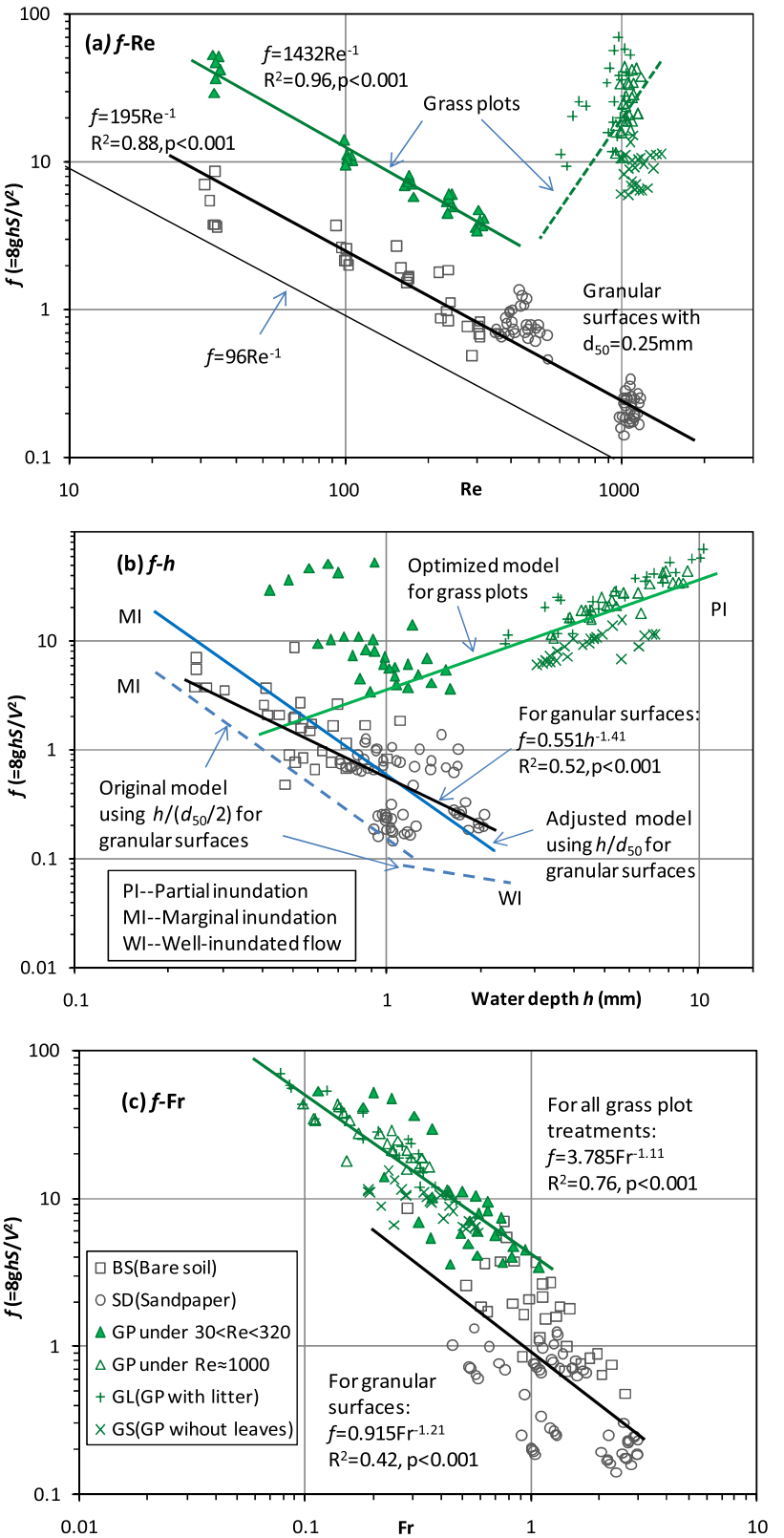

Figure 10. The resistance (a) *f*-Re, (b) *f*-*h*, and (c) *f*-Fr relation for the granular and grass plot (GP) surfaces at varying slopes (In Figure 10b, *f* was predicted based on the inundation ratio ($h/(d_{50}/2)$) of the *Lawrence* [1997] model.).

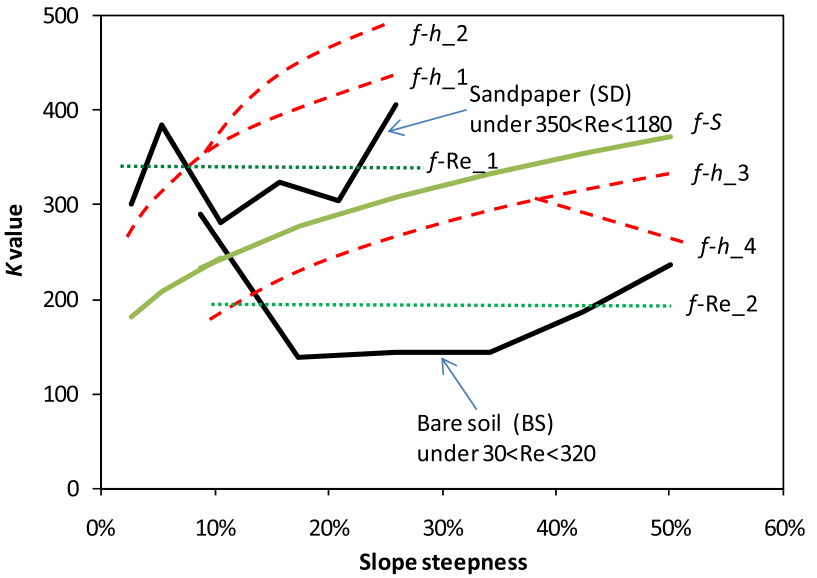

Figure 11. The fitted *K* values in Figure 3 and 4 versus slope steepness *S* for the granular surfaces. The *f*-*S* curve is calculated by $K/96 = 1+D_{90}^{1.25}S^{0.4}/263$ in a laminar flow regime [*Savat*, 1980]; The dotted lines (*f*-Re_1∼2) represent the *f*-Re relation using $f=K\mathrm{Re}^{-1}$; the dashed lines (*f*-*h*_1∼4) were predicted by *Lawrence* [1997] model, which includes three submodels based on the inundation ratio ($h/(d_{50}/2)$), in which *f*-*h*_1 and *f*-*h*_2 are predicted by the "Rough flow" and "Mixed length" sub-model, respectively, and *f*-*h* _3 and *f*-*h* _4 are predicted by the "Mixed length" and "Drag force" sub-model, respectively.

inundation (PI, $h/(d_{50}/2)\leq 1$), a mixed length submodel for marginal inundation (MI, $1<h/(d_{50}/2)<10$), and a rough flow submodel for well-inundated flow (WI, $h/(d_{50}/2)\geq 10$). The $h/(d_{50}/2)$ varied from 16.4 to 5.6 for SD, and from 8.8 to 2 for BS. So the "Rough flow" and "Mixing length" submodels are applied to predict *f*, and the models greatly underestimate *f* (original model for granular surfaces in Figure 10b). If the inundation ratio $h/(d_{50}/2)$ is replaced with h/d_{50}, the "Mixing length" submodel would more effectively predict *f* (adjusted prediction for granular surfaces in Figure 10b).

The *f* calculated by the *Lawrence* model increases with increasing *S* (*f*-*h* dashed lines in Figure 11). The decrease in $h/(d_{50}/2)$ with increasing *S* could partly explain the increasing tendency of *f* at $S>10.5\%$ for SD, and at $S>18.7\%$ for BS. The curves of *f*-*h*_2 and *f*-*h*_4 in Figure 11 also appear to be possible when the threshold inundation ratio alters slightly (i.e., 2 or 5). Nonetheless, all of the possibilities in the f-$h/(d_{50}/2)$ relation cannot explain the greater *f* at the gentle slopes.

The f_{rain} may give an explanation to the greater *f* at gentle slopes than at steep slopes. For the granular surfaces, *h* varied from 0.2 to 2.1 mm (Table 4), and the raindrop diameters mainly ranged from 1 to 2 mm. The f_{rain} at gentle slopes would be an in-negligible contributor to *f*, and its contributor tends to weaken with increasing *S* [*Shen and Li*, 1973; *Savat*, 1977; *Kinnell*, 1991]. Nonetheless, it still cannot explain the greater *f* at the 5.2% slope than at the 2.6% slope for SD (Figure 2).

Another additional resistance would be derived from roll waves. In fact, for SD, obvious roll waves appeared on all slopes except for 2.6%. Some work has also testified that roll waves commonly occur in overland flow, especially on steep hillslopes [*Emmett*, 1970; *Lu and Li*, 2002; *Liu et al*., 2005], and they related to Fr [*Julien and Hartley*, 1986]. *Hirsch* [1996] even suggested that roll waves become a main contributor to *f* under high Fr (i.e., Fr>0.6). For SD, It is interesting that no visible roll wave occurred at the 2.6% slope, but the 5.2% slope generated a larger wave height (0.46 mm under $350<\mathrm{Re}<550$ and 1.06 mm under $\mathrm{Re}\approx 1000$) than the other slopes (10.5–25.9%). If the difference in *f* between the 2.6% and 5.2% slopes represents f_{wave}, it accounts for a quarter of the total resistance at the 5.2% slope, which can also explain the greater *K* value for SD than for BS (330 versus 190, Figure 11).

Fr generally increased with increasing *S* for the granular surfaces. For BS, 25.9% is the threshold slope separating subcritical flows (i.e., Fr<1) from supercritical (i.e., Fr>1) flow regimes; and for SD, the threshold slope is 10.5%. It is a coincidence that the 25.9% and 10.5% slopes corresponded to the minimum *f* value for BS

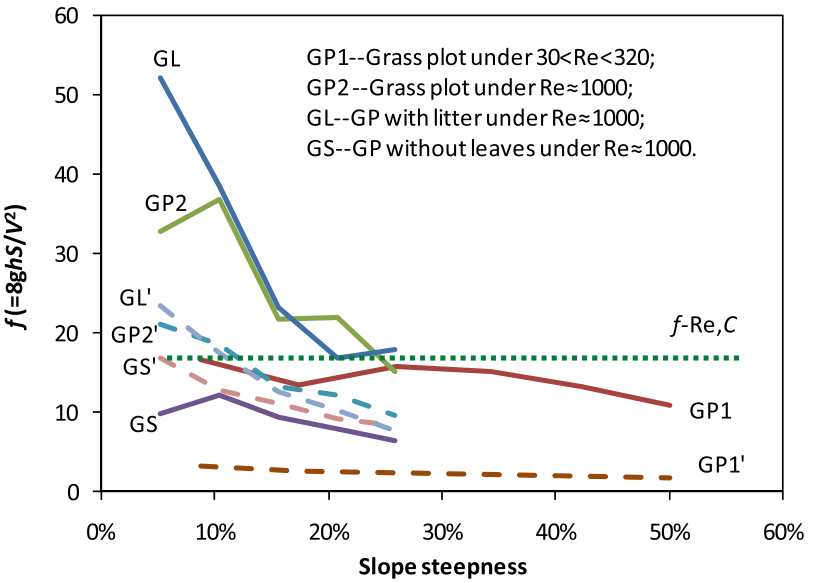

Figure 12. Resistance *f* versus slope steepness *S* for each grass treatment. The dotted level *f*-Re, *C* line represents schematic resistance *f* predicted by Re and the fractional cover (*C*) of the ground surface covered by stems, leaves, and litter; and the superscript 'denotes the calculated *f* using the "Drag force" submodel suggested by *Lawrence* [1997].

and for SD, respectively (Figure 2). It hints that *f* would decrease with *S* under subcritical flow regimes, and increase with *S* under supercritical flows.

However, unfortunately, there is limited information on the effect of flow regimes and roll waves on *f*. They are also important to soil erosion processes on steep loess slopes [*Lu and Li*, 2002; *Liu et al*., 2005]. Therefore, it is worth conducting further experiments on them for overland flows.

To sum up, on granular surfaces, although Re can well predict the resistance (Table 7 and Figure 10a), the independent variables Re, *S*, and h/d_g cannot explain the variation in *f* with *S*. The roll waves and flow regimes would give important implications to the resistance formation.

4.2.2. Grass Plots

For the grass plot treatments with Re≈1000, *S* had a significantly negative correlation with *f*, but no relation with *f* when 30<Re<320 (Table 5 and Figure 3). *Abrahams et al.* [1994] and *Hirsch* [1996] suggested that f_{grain} was calculated by equation (2), and f_{stems}, f_{leaves}, and f_{litter} positively correlated with the fractional cover (*C*) of the ground surface covered by grass stems, leaves, and litter. So *S* cannot lead to the variation in *f* for each treatment under the same Re condition (the dotted *f*-Re, *C* line in Figure 12), which disagrees with the negative *f*-*S* relation for GS, GP2, and GL (Figure 12). Meanwhile, on the grass plots, a greater *f* occurred with Re≈1000 than when 30<Re<320, which also does not correspond with the common recognition of a negative *f*-Re relation. These results imply that the resistance model based on Re, *C* may be invalid when *S* or/and Re changes greatly for vegetated slopes.

The negative *f*-*S* relation for the grass plot treatments can relate with the inundation ratio ($h/(d_{50}/2)$). *Lawrence* [1997] suggested that *f* increases with the inundation ratio based on the "Drag force" submodel for PI when *h* is much shallower than the predominant grass stem height (>3 cm) (i.e., $h/(d_{50}/2)<1$, Figure 10b). However, the parameters in the "Drag for" sub-model, such as coefficient of drag and the projected frontal area exposed to the flow field, are difficult to define because they vary with the actual shape of the obstacles. Therefore, the optimized model for the grass plot (Figure 10b) was obtained by optimization calculation. Although there are relatively large differences between the observed and predicted *f*, they have a similar decreasing trend in the *f*-*S* relation (Figure 12). The differences also highlight the importance of grass leaves and litter to *f*. However, for GP under 30<Re<320, *f* decreases with increasing *h* or $h/(d_{50}/2)$ (Figure 10b), so the "Drag force" submodel loses its efficiency. The above results indicate that for vegetated slopes, the "Drag force" submodel should be more suitable to mirror the resistance mechanism under higher Re or *h* conditions (e.g., *h*>2 mm).

Generally, the model based on Re and the fractional cover (C) is difficult to mirror the effect of S on f; and the "Drag force" submodel based on inundation ratio can capture the f-S variation trend, but its effectiveness mainly depends on the range of water depth and the assigned model parameters.

4.3. The Importance of Regrassed Slopes to Runoff and Erosion Dynamics

Compared to the granular surfaces, the grass plots significantly increased f to overland flow (Figure 10a). The contribution of grain resistance to grass plot was approximately 20% under $30<Re<320$ and 1% under $Re\approx1000$. *Abrahams and Parsons* [1991] and *Abrahams et al*. [1994] also highlighted the importance of surface standing components to total resistance when $1000<Re<5000$. They found that the grain resistance always contributes less than 10% for desert pavement slopes and for grassland and shrubland, Walnut Gulch, southern Arizona. *Prosser et al*. [1995] suggested that over 90% of flow resistance is exerted on plant stems for a well-covered grassland when $Re>10{,}000$. In this study, if Re continuously increases ($Re>1000$), f_{grain} may decrease in the laminar flow regime, or almost keep a constant with a small value in the turbulent regime, but f on grass plots may increase due to the increasing inundated water depth (Figure 10b). Therefore, the f_{grain} will be always negligible for the grass plot. However, the negligible proportion of f_{grain} may be attributed to the plane granular bed surface.

When $Re\approx1000$, the resistance of grass plot is 40–160 times as much as that of the granular surface (Figure 7b), which means that the former flow velocity would be 1/5–1/3 of the latter according to equation (1). Therefore, revegetation will significantly prolong runoff duration from slopes to gullies or rivers [*Emmett*, 1970]. Additionally, vegetation cover can also strengthen soil infiltration capacity and prolong the time to runoff [*Morgan et al*., 1997; *Jiang*, 1997; *Pan and Shangguan*, 2006]. Consequently, revegetation could cut down the flood peak discharge and influence the delivery of nutrients (e.g., nitrogen) in watersheds [*Zhang et al*., 2008; *Alexander et al*., 2000].

Compared to the grass plots, the greater bed shear stress (15–35 times) on the bare soil is bound to increase the possibility of erosion occurrence (Figure 8b), even though the effect of vegetation roots in strengthening the soil cohesion has not be considered. This finding supports that vegetation can decrease an order magnitude difference in soil loss rates compared with bare soil plot [*Pierson et al*., 1994; *Hou and Du*, 1985; *Pan et al.,* 2006]. On the loess plateau of China, with the implementation of the "Grain for Green" project, vegetation has been widely restored in recent years. This finding also supports an explanation to the sharp drop in the sediment yield produced from the middle reaches of Yellow River [*Liu et al*., 2015].

The bed shear stress of the grass plot under $Re\approx1000$ was even smaller than that under $30<Re<320$ (Figure 8). This may be attributed to the increase in inundated water depth, and more runoff energy dissipates against the grass components under the relatively high Re (Figure 10b). On arid or semiarid areas, due to the rainfall runoff gathering effect, the downslope tends to correspond to a higher flow discharge or Re than the upslope [*Jiang*, 1997]. Therefore, the effect of revegetation on runoff and erosion dynamics may become more significant on downslope than on upslope, which further mirrors the importance of vegetation spatial distribution. *Cerdà* [1998] conducted simulated rainfall experiments to investigate the runoff and erosion behavior at different slope positions, and suggested that vegetation is the most important factor determining the soil erosion and runoff rates within the slope. However, *Prosser et al*. [1995] found that when Re exceeded 10,000, the bed shear stress of grassland increased with increasing Re. The Prosser's finding as well as our results indicates that for vegetated slopes, a threshold slope length may exist where Re corresponds to the minimum bed shear stress, and the effectiveness of vegetation in controlling hillslope soil erosion may be associated with vegetation spatial distribution and rainfall-runoff characteristics.

When $Re\approx1000$, the contribution of grass leaves, stems, litter, and soil grain to the total resistance were approximately 52%, 31%, 16%, and 1%, respectively. Because such a great contribution (>80%) derives from leaves and stems, from the perspective of flood control, it would be better to avoid harvesting grass or grazing pastures in flood period. This result highlights the importance of grass leaves, which are frequently ignored in overland flow resistance as some leaves are untouched by the flow [*Thompson et al*., 2004]. A possible reason for the greater f_{leaves} is that the soft grass leaves impacted by raindrop impact were lodging on the plot surface. This finding would generalize to the other well-covered grass species with soft stems and leaves. It further implies that although it is recognized that vegetation cover has important effects on overland runoff processes, the impact of grass leaves or cover would differ from shrubs or forest stands [*Wainwright et al*, 1999]. The ryegrass in this study was in the tillering and jointing stages, and the

grass strips were well formed with a relatively high cover. As the perennial grass continuously developed, the accumulated litter would neutralize the importance of leaves to total resistance. A decrease in grass cover or leaf area index would lower the efficiency of grass restoration in controlling soil erosion on hillslope, and the spatial distribution of grass should also be paid attention to due to its possible effect on overland flow path [*Pan and Shangguan*, 2006; *Abrahams et al.*, 1994].

5. Conclusions

Experiments on hydraulic resistance to overland flow on the granular and grass plot surfaces under simulated rainfall and inflow conditions were conducted, and the resistance at varying slopes and its portioning on the grass plots were discussed. On upslope of a hillslope, the resistance f in both the granular and grass plot surfaces gradually decreases with the downward cross sections, and there is a good relationship between f and Re. This indicates that the observed f based on a small-size runoff plot under rainfall conditions would be overestimated, and it would be better to observe Vs or h on downslope. However, the effect of plot size on f may weaken on field hillslopes due to the irregular surface microtopography.

For the granular surfaces, the greater f occurred at the gentle and steep slopes, and there existed a threshold S (i.e., 10–25%) that corresponded to the minimum f. Coincidently, the threshold of S also divided into two flow regimes based on Fr values (i.e., Fr$>$1 or Fr$<$1), and f decreased with S under the subcritical flows and increased with S under supercritical flows. The resistance f on the grass plot treatments decreased with increasing S when Re$\approx$1000, which differs from the f-S relation on the granular surfaces. This indicates that revegetation changes the variation in f with S, and that S is not an independent variable in predicting f on different hillslopes.

Re is a good variable to predict f for regular granular slopes, and Fr is more suitable to estimate f for vegetated slopes. The variation in f with S is difficult to be captured by the popular resistance models. Therefore, further investigations on the resistance formation mechanism are required to predict hydrological or soil erosion processes on hillslopes.

When Re$\approx$1000, the f in the grass plot with 70% cover was 40–160 times as much as that on the granular surface, and the former bed shear stress was only 3–6% of the latter. The contribution of grass-plot components to total resistance follows grass leaves$>$stems$>$litter$>$soil grain, and grain resistance is negligible ($<$1%). The greater resistance contribution caused by grass leaves (approximately 52%) may be attributed to the leaves touching the plot surface impacted by raindrop impact. Compared with the granular slopes, the grassed slopes significantly increases f to overland flow and decreases flow velocity. Therefore, vegetation restoration will prolong time to slope runoff generation and concentration and decrease flood peak discharge in river channels. Meanwhile, grass plantation largely reduces the bed shear stress impacting soil erosion. This hints that revegetation will greatly decrease the potential of soil erosion even if the strengthening effect of vegetation roots on the soil critical shear stress is not considered. This finding matches the sharp drop in the sediment yield generated from the middle reaches of Yellow River due to the vegetation restoration in recent years.

Notation

BS	Bare soil plots covered with 0.25 mm height naturally grown moss
SD	Sandpaper surface with grain diameter of 0.25 mm, including SD1 for 350$<$Re$<$550 and SD2 for 980$<$Re$<$1180
GP	Grass plots without litter, including GP1 for 30$<$Re$<$320, and GP2 for 960$<$Re$<$1180
GL	Grass plots with additional litter
GS	Grass plots without leaves
CSS	The cross section measuring surface flow velocity and water depth
d_{50}	Grain median diameter, mm
S	Slope steepness, %
q	Flow rate per unit width, $m^2\ s^{-1}$
h	Water depth, m
Vs	The measured surface flow velocity using dying tracer method, $m\ s^{-1}$

V	Mean flow velocity calculated by the volumetric relation ($V = q/h$), m s^{-1}
α	Correction factor in determining mean velocity ($\alpha = V/Vs$)
Re	Flow Reynolds number, Re $= 4Vh/\upsilon$ (υ *is* the kinematic viscosity)
Fr	Froude number, Fr $= V/(gh)^{0.5}$ (*g is* the acceleration due to gravity)
f	Darcy-Weisbach resistance to overland flow
K	The fitted value using the equation $f = KRe^{-1}$, representing friction roughness
f_{grain}	The resistance derived from granular bed
f_{litter}	The hydraulic resistance derived from grass litter
f_{stems}	The hydraulic resistance derived from grass stems
f_{leaves}	The hydraulic resistance derived from grass leaves

Acknowledgments
This research was jointly funded by the National Natural Science Foundation of China Project (grants 41271285, 51309007, 41530858), and the Fundamental Research Funds for the Central Universities and Beijing Higher Education Young Elite Teacher Project. The experimental data in this study have been acquired with the help of some anonymous workers. Some data are listed in the tables in the manuscript; any additional data may be obtained from C. Z. Pan (email: pancz@bnu.edu.cn). The authors would like to express deep gratitude to the reviewers for their constructive comments and helpful suggestions on the manuscript.

References

Abrahams, A. D., and A. J. Parsons (1991), Resistance to overland flow on desert pavement and its implications for sediment transport modeling, *Water Resour. Res.*, *27*, 1827–1836.
Abrahams, A. D. and A. J. Parsons (1994), Hydraulics of interrill overland flow on stone-covered desert surfaces, *Catena*, *23*, 111–140.
Abrahams, A. D., A. J. Parsons, and S. H. Luk (1986), Resistance to overland flow on desert hillslopes, *J. Hydrol.*, *50*, 343–363.
Abrahams, A. D., A. J. Parsons, and J. Wainwright (1994), Resistance to overland flow on semiarid grassland and shrubland hillslopes, Walnut Gulch, southern Arizona, *J. Hydrol.*, *156*, 431–446.
Alexander, R. B., R. A. Smith, and G. E. Schwarz (2000), Effect of stream channel size on the delivery of nitrogen to the Gulf of Mexico, *Nature*, *403*, 758–761, doi:10.1038/35001562.
Atkinson, J. F., A. D. Abrahams, C. Krishnan, and G. Li (2000), Shear stress partitioning and sediment transport by overland flow, *J. Hydraul. Res.*, *38*, 37–40.
Cerdà, A. (1998), The influence of geomorphological position and vegetation cover on the erosional and hydrological processes on a Mediterranean hillslope, *Hydrol. Processes.*, *12*, 661–671.
Chow, V. T. (1959), *Open-Channel Hydraulics*, 679 pp., McGraw-Hill, N. Y.
Emmett, W. W. (1970), The hydraulics of overland flow on hillslopes, *U.S. Geol. Surv. Prof. Pap.*, *662-A*, A-1-–A-68.
Fox, D. M., and R. B. Bryan (2000), The relationship of soil loss by interrill erosion to slope gradient, *Catena*, *38*(3), 211–222, doi:10.1016/S0341-8162(99)00072-7.
Gabarrón-Galeote, M. A., J. F. Martínez-Murillo, M. A. Quesada, and J. D. Ruiz-Sinoga (2013), Seasonal changes in the soil hydrological and erosive response depending on aspect, vegetation type and soil water repellency in different Mediterranean micro environments, *Solid Earth*, *4*, 497–509, doi:10.5194/se-4-497-2013.
Gilley, J. E., and S. C. Finkner (1991), Hydraulic roughness coefficients as affected by random roughness, *Trans. ASAE*, *34*(3), 897–903.
Gilley, J. E., and E. R. Kottwitz (1994), Darcy-Weisbach roughness coefficients for selected crops, *Trans. ASAE*, *37*(2), 467–471.
Gilley, J. E., D. C. Flanagan, E. R. Kottwitz, and M. A. Weltz (1992), Darcy-Weisbach roughness coefficients for overland flow, in *Overland Flow Hydraulics and Erosion Mechanics*, edited by A. J. Parsons and A. D. Abrahams, pp. 25–52, UCL Press, London, U. K.
Hirsch, P. J. (1996), Hydraulic resistance to overland flow on semiarid hillslopes: A physical simulation, PhD dissertation, State Univ. of New York at Buffalo, Buffalo.
Holden, J., M. J. Kirkby, S. N. Lane, D. G. Milledge, C. J. Brookes, V. Holden, and A. T. McDonald (2008), Overland flow velocity and roughness properties in peatlands, *Water Resour. Res.*, *44*, W06415, doi:10.1029/2007WR006052.
Horton, R. E., H. R. Leach, and R. Van Vliet (1934), Laminar sheet flow, *Trans. AGU*, 2, 393–404.
Hou, X. L., and C. X. Du (1985), Runoff and soil loss under different vegetation cover plots [in Chinese with English abstract], *Soil Conserv. Bull.*, *5*, 35–37.
Jiang, D. S. (1997), *Soil loss and its controlling mode on the loess plateau [in Chinese with English abstract]*, China's Water Conserv. and Hydropowe Press, Beijing.
Julien, P. Y., and D. M. Hartley (1986), Formation of roll-waves in laminar sheet flow, *J. Hydraul. Res.*, *24*(1), 5–17.
Kim, J., V. Y. Ivanov, and N. D. Katopodes (2012), Hydraulic resistance to overland flow on surfaces with partially submerged vegetation, *Water Resour. Res.*, *48*, W10540, doi:10.1029/2012WR012047.
Kinnell, P. I. A. (1991), The effect of flow depth on sediment transport induced by raindrops impacting shallow flows, *Trans. ASAE*, *34*, 161–168.
Lawrence, D. S. L. (1997), Macroscale surface roughness and frictional resistance in overland flow, *Earth Surf. Processes Landforms*, *22*(4), 365–382.
Lawrence, D. S. L. (2000), Hydraulic resistance in overland flow during partial and marginal surface inundation: Experimental observations and modeling, *Water Resour. Res.*, *36*, 2381–2393.
Liu, Q. Q., L. Chen, J. C. Li, V. P. Singh (2005), Roll waves in overland flow, *J. Hydrol. Eng.*, *10*(2), 110–117.
Liu, X. Y., S. T. Yang, X. Y., Li, X. Zhou, Y. Luo, and S. Z. Dang (2015), The current vegetation restoration effect and its influence mechanism on the sediment and runoff yield in severe erosion area of Yellow River Basin [in Chinese with English abstract], *Sci .Sin. Tech.*, *45*, 1052–1059, doi:10.1360/N092015-00028.
Lu, K. X., and Z. B. Li (2002), Theoretical study on formation mechanism of erosion holes of beginning of rill erosion development on loess slopes [in Chinese with English abstract], *J. Soil Water Conserv.*, *16*(1), 35–38.
Ma, L., C. Z. Pan, Y. G. Teng, and Z. P. Shangguan (2013), The performance of grass filter strips in controlling high-concentration suspended sediment from overland flow under rainfall/non-rainfall conditions, *Earth Surf. Processes Landforms*, *38*, 1523–1534.
Morgan, R. P. C. (1986), *Soil Erosion and Conservation*, Longman Group UK Ltd, Harlow, U. K.
Morgan, R. P. C., K. McIntyre, A. W. Vickers, J. N. Quinton, and R. J. Rickson (1997), A rainfall simulation study of soil erosion on rangeland in Swaziland, *Soil Technol.*, *11*(3), 291–299, doi:10.1016/S0933-3630(97)00013-5.
Pan, C. Z., and Z. P. Shangguan (2006), Runoff hydraulic characteristics and sediment generation in sloped grass plots under simulated rainfall conditions, *J. Hydrol.*, *331*, 178–185.

Pan, C. Z., and Z. P. Shangguan (2007), Hydraulic characteristics of silt-laden flow on different gradient grass plots and its mechanism of sediment retention [in Chinese with English abstract], *Adv. Water Sci.*, *18*(4), 490–495.
Pan, C. Z., Z. P. Shangguan, and T. W. Lei (2006), Influences of grass and moss on runoff and sediment yield on sloped loess surfaces under simulated rainfall, *Hydrol. Processes*, *20*, 3815–3824.
Pan, C. Z., L. Ma, and Z. P. Shangguan (2010), Effectiveness of grass strips in trapping suspended sediments from runoff, *Earth Surf. Processes Landforms*, *35*, 1006–1013.
Parsons, A J., A. D. Abrahams, and J. Wainwright (1994), On determining resistance to interrill overland flow, *Water Resour. Res.*, *30*, 3515–3521.
Parsons, A. J., J. Wainwright, A. D. Abrahams, and J. R. Simanton (1997), Distributed dynamic modelling of interrill overland flow, *Hydrol. Processes*, *11*(14), 1833–1859.
Pierson, F. B., Jr., S. S. van Vactor, W. H. Blackbum, and J. C. Wood (1994), Incorporating small scale spatial variability into predictions of hydrologic response on sagebrush rangelands, in *Variability in Rangeland, Water Erosion Processes, Soil Sci. Soc. Am. Spec. Publ.*, vol. 38, edited by W. H. Blackbum, pp. 23–34, Soil Science Society of America, Madison, Wis.
Prosser, I. P., W. E. Dietrich, and J. Stevenson (1995), Flow resistance and sediment transport by concentrated overland flow in a grassland valley, *Geomorphology*, *13*, 71–86.
Rauws, G. (1988), Laboratory experiments on resistance to overland flow due to composite roughness, *J. Hydrol.*, *103*, 37–52.
Roels, J. M. (1984), Flow resistance in concentrated overland flow on rough slope surfaces, *Earth Surf. Processes Landforms*, *9*, 541–551.
Savat, J. (1977), The hydraulics of sheet flow on a smooth surface and the effect of simulated rainfall, *Earth Surf. Processes Landforms*, *2*, 125–140.
Savat, J. (1980), Resistance to flow in rough supercritical sheet flow, *Earth Surf. Processes Landforms*, *5*, 103–122, doi:10.1002/esp.3760050202.
Sha, Y. Q. (1965), *An Introduction to the Mechanics of Sediment Transport*, China Ind. Press, Beijing.
Shen, H. W., and R. M. Li (1973), Rainfall effects on sheet flow over smooth surface, *J. Hydraul. Div. Am. Soc. Civ. Eng.*, *99*(5), 771–792.
Smith, M. W., N.J. Cox, and L. J., Bracken (2007), Applying flow resistance equations to overland flows, *Prog. Phys. Geogr.*, *31*, 363–387.
Takken, I., and G. Govers (2000), Hydraulics of interrill overland flow on rough, bare soil surfaces, *Earth Surf. Processes Landforms*, *25*, 1387–1402.
Thompson, A. M., B. N. Wilson, and B. J. Hansen (2004), Shear stress partitioning for idealized vegetated surfaces, *Trans. ASAE*, *47*(3), 701–709.
Wainwright, J., A. J. Parsons, and A. D. Abrahams (1999), Rainfall energy under creosotebush, *J. Arid Environ.*, *43*, 111–120.
Wainwright, J., Parsons, A. J., and A. D. Abrahams (2000), Plot-scale studies of vegetation, overland flow and erosion interactions: Case studies from Arizona and New Mexico, *Hydrol. Processes*, *14*(5), 2921–2943.
Weltz, M. A., A. B. Arslan, and L. J. Lane (1992), Hydraulic roughness coefficients for native rangelands, *J. Irrig. Drain. Eng.*, *118*(5), 776–790.
Xu, X. Z., D. Q. Liu, H. W. Zhang, Z. D. Dong, and M. D. Zhu (2006), Laboratory rainfall simulation with controlled rainfall intensity and drainage [in Chinese with English abstract], *J. Beijing For. Univ.*, *28*(5), 52–58.
Zhang, J. J., L., Na, H. B. Dong, and P. Wang (2008), Hydrological response to changes in vegetation covers of small watersheds on the Loess Plateau [in Chinese with English abstract], *Acta Ecol. Sin.*, *28*(8), 3597–3605.